C2SMART
CONNECTED CITIES WITH SMART TRANSPORTATION
A USDOT University Transportation Center

New York University
Rutgers University
University of Washington
University of Texas at El Paso
The City College of New York

Integration and Operation of an Advanced Weigh-in-Motion (A-WIM) System for Autonomous Enforcement of Overweight Trucks

September 2022

TECHNICAL REPORT DOCUMENTATION PAGE

1. Report No.	2. Government Accession No.	3. Recipient's Catalog No.
4. Title and Subtitle Integration and Operation of an Advanced Weigh-in-Motion (A-WIM) System for Autonomous Enforcement of Overweight Trucks		5. Report Date September 2022 6. Performing Organization Code:
7. Author(s) Hani Nassif, Kaan Ozbay, Chaekuk Na, Peng Lou		8. Performing Organization Report No.
9. Performing Organization Name and Address Connected Cities for Smart Mobility towards Accessible and Resilient Transportation Center (C2SMART), 6 Metrotech Center, 4th Floor, NYU Tandon School of Engineering, Brooklyn, NY, 11201, United States		10. Work Unit No. 11. Contract or Grant No. 69A3551747119
12. Sponsoring Agency Name and Address Office of Research, Development, and Technology Federal Highway Administration 6300 Georgetown Pike McLean, VA 22101-2296		13. Type of Report and Period Final report: 03/01/21-09/30/22 14. Sponsoring Agency Code
15. Supplementary Notes		

16. Abstract
The ultimate objective of this project is to assist and support the NYCDOT in establishing the legislation to operate the autonomous OW enforcement system and extend the service life of the BQE corridor. This project evaluates the effectiveness of the implemented enforcement system. The report first presents the work on the existing advanced weight-in-motion system (A-WIM) and proposed new A-WIM system, as well as the automated license plate recognition (ALPR) system. A new structural health monitoring (SHM) system was also implemented in the testbed to evaluate the responses of structures under the traffic. Then evaluations of the multiple systems in the testbed are presented by presenting the results of accuracy of different weighing sensors, and practices of automated enforcement. Lastly, reliability-based live load factors for bridge load rating are developed.

17. Key Words	18. Distribution Statement No restrictions. This document is available to the public through the National Technical Information Service, Springfield, VA 22161. http://www.ntis.gov		
19. Security Classif. (of this report) Unclassified	20. Security Classif. (of this page) Unclassified	21. No. of Pages 50	22. Price

Form DOT F 1700.7 (8-72) Reproduction of completed page author

C2SMART Center is a USDOT Tier 1 University Transportation Center taking on some of today's most pressing urban mobility challenges. Using cities as living laboratories, the center examines transportation problems and field tests novel solutions that draw on unprecedented recent advances in communication and smart technologies. Its research activities are focused on three key areas: Urban Mobility and Connected Citizens; Urban Analytics for Smart Cities; and Resilient, Secure and Smart Transportation Infrastructure.

Some of the key areas C2SMART is focusing on include:

Disruptive Technologies

We are developing innovative solutions that focus on emerging disruptive technologies and their impacts on transportation systems. Our aim is to accelerate technology transfer from the research phase to the real world.

Unconventional Big Data Applications

C2SMART is working to make it possible to safely share data from field tests and non-traditional sensing technologies so that decision-makers can address a wide range of urban mobility problems with the best information available to them.

Impactful Engagement

The center aims to overcome institutional barriers to innovation and hear and meet the needs of city and state stakeholders, including government agencies, policy makers, the private sector, non-profit organizations, and entrepreneurs.

Forward-thinking Training and Development

As an academic institution, we are dedicated to training the workforce of tomorrow to deal with new mobility problems in ways that are not covered in existing transportation curricula.

Led by the New York University Tandon School of Engineering, C2SMART is a consortium of five leading research universities, including Rutgers University, University of Washington, the University of Texas at El Paso, and The City College of New York.

c2smart.engineering.nyu.edu

Integration and Operation of an Advanced Weight-In-Motion (WIM) System for Autonomous Enforcement of Overweight Trucks

Hani Nassif, PE, PhD
Principal Investigator
Rutgers University, New Jersey

Kaan Ozbay, PhD
Co PI
New York University, New York

Peng Lou, PhD
Research Associate
Rutgers University, New Jersey

Chaekuk Na, PhD
Research Associate
Rutgers University, New Jersey

Disclaimer

The contents of this report reflect the views of the authors, who are responsible for the facts and the accuracy of the information presented herein. This document is disseminated in the interest of information exchange. The report is funded, partially or entirely, by a grant from the U.S. Department of Transportation's University Transportation Centers Program. However, the U.S. Government assumes no liability for the contents or use thereof.

Acknowledgments

The authors would like to acknowledge the financial support of C2SMART (Connected Cities for Smart Mobility toward Accessible and Resilient Transportation) Tier 1 University Transportation Center at New York University. The authors also would like to thank the New Jersey Turnpike Authority to offer the cost-sharing fund for this study. The authors would like to thank the New York City Department of Transportation (NYCDOT) and New Jersey Department of Transportation (NJDOT) that provided the databases required for the successful completion of this project.

Executive Summary

Roadways in New York City handle substantial daily traffic throughout different boroughs. Trucks have been an integral part of the freight movement network in distributing goods and services to various communities; however, many trucks are often overloaded beyond legal load limits. The Brooklyn-Queens Expressway (BQE) that connects two boroughs suffers from significant deterioration because of the existing environmental conditions exacerbated by a substantial number of OW trucks. From the previous studies, the team learned that the average daily number of OW trucks on BQE is significantly higher, and the extent of the OW (or OW tonnage) is substantially heavier than the national average. The team also found that current OW enforcement practices at the weighing stations and by the weight enforcement officers using portable scales would capture only a small fraction of the OW trucks. Therefore, a more practical and efficient OW enforcement scheme would be needed to discourage the trucking industry from overloading its fleets.

The ultimate objective of this project is to assist and support the NYCDOT in establishing the legislation to operate the autonomous OW enforcement system and extend the service life of the BQE corridor. This project evaluates the effectiveness of the implemented enforcement system. The report first presents the work on the existing advanced weight-in-motion system (A-WIM) and proposed new A-WIM system, as well as the automated license plate recognition (ALPR) system. A new structural health monitoring (SHM) system was also implemented in the testbed to evaluate the responses of structures under the traffic. Then evaluations of the multiple systems in the testbed are presented by presenting the results of accuracy of different weighing sensors, and practices of automated enforcement. Lastly, reliability-based live load factors for bridge load rating are developed.

Table of Contents

List of Figures

List of Tables

Section 1 – Introduction

Roadways in New York City handle substantial daily traffic throughout different boroughs. Trucks have been an integral part of the freight movement network in distributing goods and services to various communities; however, many trucks are often overloaded beyond legal load limits. The Brooklyn-Queens Expressway (BQE) that connects two boroughs suffers from significant deterioration because of the existing environmental conditions exacerbated by a substantial number of OW trucks. The New York City Department of Transportation (NYCDOT) has been planning to rehabilitate the bridge to accommodate future traffic volume and weight demands. Accordingly, the team closely worked with the NYCDOT and collected truck traffic and weight data to provide recommendations for future design or rehabilitation work on BQE bridges. The team learned that the average daily number of OW trucks is significantly higher, and the extent of the OW (or OW tonnage) is substantially heavier than the national average. Our team also found that current OW enforcement practices at the weighing stations and by the weight enforcement officers using portable scales would capture only a small fraction of the OW trucks. For example, the number of vehicles screened by four weighing stations in NJ was 1,006,749 in 2009, and only 0.142% (1,430 trucks) of screened trucks were overweighted and ticketed. However, the actual OW percentage along the corridors near four weighing stations in NJ was 6.4%, based on the WIM data. This confirms that the current OW enforcement practices would only capture less than 3% of total OW trucks. Therefore, a more practical and efficient OW enforcement scheme would be needed to discourage the trucking industry from overloading its fleets.

The ultimate objective of this project is to assist and support the NYCDOT in establishing the legislation to operate the autonomous OW enforcement system and extend the service life of the BQE corridor. The team has implemented the first testbed and made the plan for a new testbed on both sides of the BQE corridor to develop the guidelines and specifications for the operation of the OW enforcement system in an urban area.

This report aims to utilize the existing testbed to develop an effective autonomous enforcement system of overweight trucks by integrating various technologies, including an advanced weight-in-motion (A-WIM) system and an automated license plate recognition system. In addition, a comprehensive structural health monitoring system has been implemented to monitor the structure's conditions. Data from both A-WIM and SHM are evaluated and investigated to reflect the impact of overweight trucks on the infrastructure. This report first elaborates on establishing a new smart roadway testbed at the south part of the BQE corridor. The smart roadway testbed consists of two major systems, one system to capture the information of trucks including the configuration, weight, and license plate, and the other system to capture the responses of the structure under the trucks. A statistical correlation of data from A-WIM and SHM is presented. Then the evaluation of the smart roadway testbed is performed. A comparison of truck measurement data from different types of weighing sensors is presented. The accuracy of weighing sensors is of critical to establishing the autonomous enforcement system. Then the

integration of A-WIM and automated license plate recognition (ALPR) data is performed. The accuracy of the matching algorithm is evaluated. In the end, recommendations are made to further improve the accuracy of the automated enforcement system.

Section 2 – Establishment of a New Smart Roadway Testbed at the South Part of the BQE Corridor

2.1. Design and Plans for A New Advanced Weight-In-Motion System in New Smart Roadway Testbed

As part of the BQE testbed developed by C2SMART, the team collaborated with NYCDOT and Kistler Instrument Corporation to establish a new smart roadway testbed at the north portion along the BQE corridor. This testbed is equipped with four Quartz sensors and two loops on the right lane of Queens bound of the BQE corridor. The Advanced Weight-In-Motion (A-WIM) system is currently monitoring the truck weights and traffic volumes to develop the autonomous enforcement scheme. In addition, this C2SMART testbed included the automated license plate recognition (ALPR) system to evaluate the performance of the ALPR system and to test the protocol to match two datasets of WIM and ALPR. Based on the lessons learned from the first testbed, the team has been working with the NYCDOT to establish another smart roadway testbed using the A-WIM system and ALPR system at the south portion along the BQE corridor. The new testbed will be equipped with 4-6 Quartz sensors per lane on all 6 lanes (3 lanes in each direction), along with an ALPR system and security cameras. Figure 1 shows the preliminary drawing of this site.

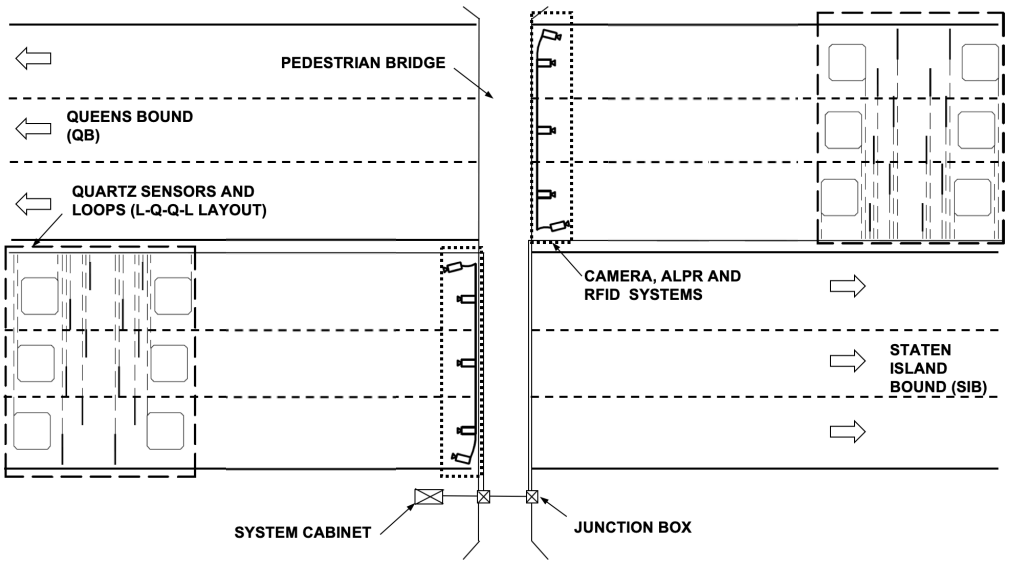

Figure 1 – New Smart Roadway Testbed at BQE

The team is currently working closely with NYCDOT, Triple Cantilever Design Joint Venture (TCDJV), and contractors to develop the specifications that will cover a selection of sensors, systems, and other peripherals, as well as the installation of various components of the system. Prior to any installation, the WIM site will be visually observed to check the pavement condition. Then the falling weight

deflectometer (FWD, see Figure 2) and surface profile tests will be performed to quantify the pavement condition. This is a critical step in selecting the most appropriate location(s) to maximize the weighing accuracy. The team will analyze the FWD and surface profile test results and assess the pavement condition. If the pavement condition is deemed to be OK, the team will recommend the pavement segment(s) for WIM installation. However, if no pavement segment would be suitable for high weighing accuracy, the team will recommend to re-work to improve the pavement conditions.

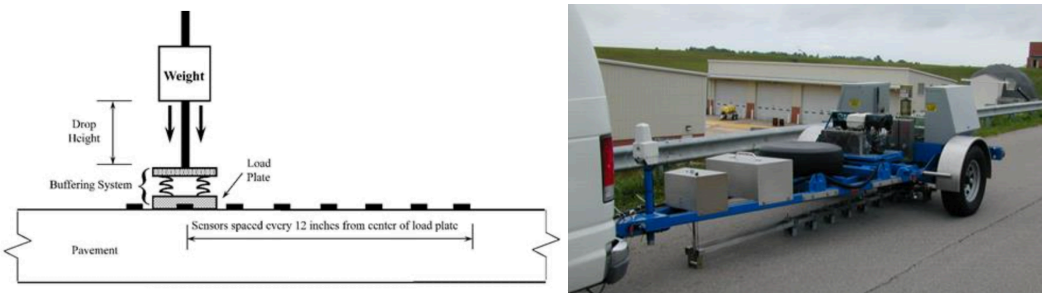

Figure 2 –FWD Testing Schematic Diagram and Dynatest® heavyweight FWD (Smith et al. 2017)

Moreover, the traffic conditions need to be considered to improve the weighing accuracy. Our partner, Kistler Instrument Corp., provides different Quartz sensor layouts that could offer less than 5% of GVW error and other features depending on traffic conditions, as shown in Figure 3. A detailed description is summarized below. The team will obtain the traffic statistics (volume, speed, etc.) from NYCDOT to select the most appropriate sensor layout to maximize the weighing accuracy. Figure 3(a) is a typical 2-row layout using 4 Quartz sensors, and it could offer less than 5% of GVW error. Figure 3(b) is a double staggered layout using 4 Quartz sensors. Similar to Figure 3(a), it also could offer less than 5% GVW error. In addition, this layout provides a stop-and-go capability to improve the accuracy during congestion. Figure 3(c) is a typical 3-row layout using 6 Quartz sensors, and as it utilizes 2 more sensors, the maximum GVW error would be 3.5%. This also provides a stop-and-go feature. Figure 3(d) has another advantage to detect single/dual tires in addition to the stop-and-go feature. However, the maximum GVW error would be slightly higher (4%) than in Figure 3(c). Figure 3(e) would provide the same features and accuracy as Figure 3(d).

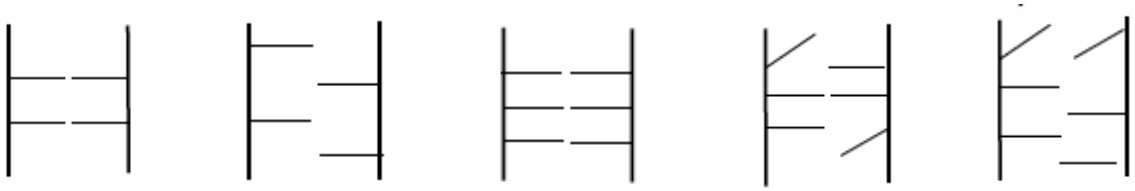

Figure 3 – Quartz Sensor Layout; (a) 2-Row, (b) Double Staggered, (c) 3-Row, (d) 6 Sensors Tilted Option 1, and (e) 6 Sensors Tilted Option 2

After instrumentation, calibration testing will be performed using a truck with a known weight or calibration truck. This calibration is an essential step to improve the system accuracy because the environmental factors, such as the depth and width of pavement cut, quality of sensor installation, quantity and quality of resin used, pavement roughness, pavement type, etc., may affect the weighing accuracy. The calibration truck shall be a Class 6/7 single unit truck with 3-4 axles or a Class 9 semi-trailer truck with 5-axle with a minimum GVW of 60 kips. Figure 4 shows an example of Class 9, 3S2 Type truck for calibration testing. The truck shall be weighed at a scale to measure each individual axle weight, tandem (or tridem) weight, and GVW, and the weighing certificates shall be provided.

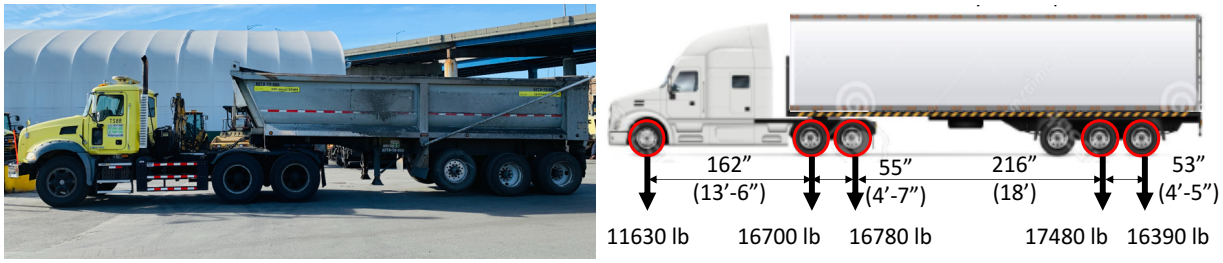

Figure 4 –Typical Class 9 Calibration Truck

2.2. Implementation of Automated License Plate Recognition system in New Smart Roadway Testbed

The automatic license plate recognition (ALPR) system has been in great demand as a useful security tool. It is still not widely deployed because it requires proprietary hardware and specially designed cameras (see Figure 5(a)) that are generally expensive. In contrast, the software-based ALPR system could work with conventional cameras on the market (non-proprietary). The costs for deployment and maintenance for the cameras and other peripherals of the SW-based ALPR would be a small fraction of the price for the proprietary ALPR system. Therefore, the team will deploy the SW-based ALPR system using typical security cameras and existing infrastructures (see Figure 5(b)) and integrate it with the A-WIM system for this project. The ALPR or camera can provide the license plate number (if permitted by legislation) or USDOT truck number, usually displayed on the side door of the truck cabin.

Several important parameters that affect the accuracy of the ALPR system are listed below, such as lighting, camera angle, image pixel, etc.

- **Lighting**: An adequate amount of light in conjunction with a faster shutter speed is critical to capture a clear image of the violated truck and its license plate. The shutter speed is crucial because it directly correlates to the image sharpness. If the shutter speed is 1/10000th of a second, the vehicle at 30 mph (avg. speed at BQE) will move 1/20th of an inch, and the image sharpness would be sufficient to capture the license plate. However, if the shutter speed is 1/1000th of a second, the vehicle at 30 mph will move 0.5 inches. In this case, the image will

result in a motion blur, and the system cannot capture the license plate. In addition, the camera requires an internal or external IR-illuminator when the amount of ambient light is not sufficient to capture vehicles. The IR-illuminator will improve image quality by removing the headlights and leaving the dimmer license plate image visible.

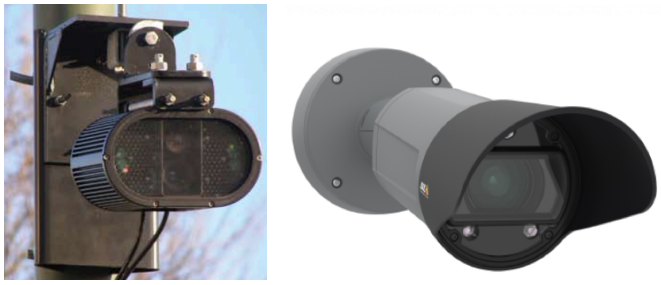

(a) (b)

Figure 5 – ALPR Cameras; (a) P382 Camera of PIP Technology (Proprietary), and (b) Q1700LE of AXIS Camera (Non-proprietary)

- **Camera Angle**: It would be best to install the camera to capture the license plate at as direct an angle as possible. However, because of the constraints of the ALPR camera installation, they are generally located at the gantry over the roadway or at the light post on the shoulder. The adequate angles in both vertical direction (as it will be installed at a certain height) and horizontal direction (if it is installed at the light post) is important. In general, an angle less than 40 degrees in both directions is required to precisely capture the license plate. Accordingly, the distance between the camera and license plate at capturing could be determined. Figure 6 shows an example with a height of 20' (gantry height at BQE). It shows that when the vehicle speed is 40 mph, the minimum distance from the camera to the license plate would be 24'.
- **Image Pixels**: The number of pixels per inch is the most critical parameter for capturing the license plate. A higher number of pixels could be achieved using a camera with higher optical zoom and resolution. In general, at least 10 pixels are required per letter or number to capture correctly. Since the US license plate has 6-7 letters and/or numbers, a minimum of 75 pixels is required for the ALPR system.

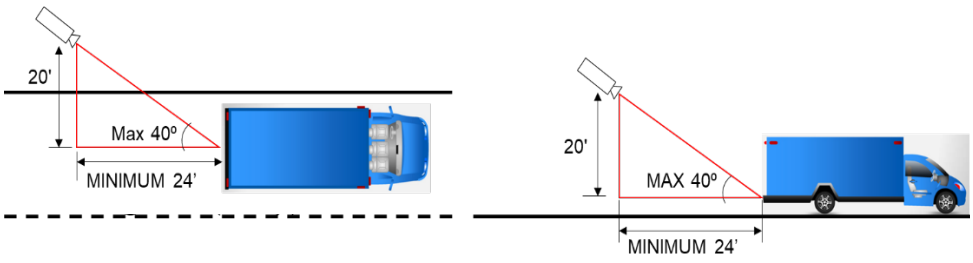

Figure 6 – Camera Angle Requirement

Based on the preliminary evaluation of the SW-based ALPR system at the first testbed on BQE, the ALPR system with the non-proprietary camera would be able to capture the license plate. Figure 7 shows the preliminary test of the ALPR system with AXIS cameras. It shows that the SW-based ALPR system could capture the license plate with ambient light and at night with the IR-illuminator. The team will test other cameras for different parameters listed above to select the adequate cameras and angles for the new smart roadway testbed in future study.

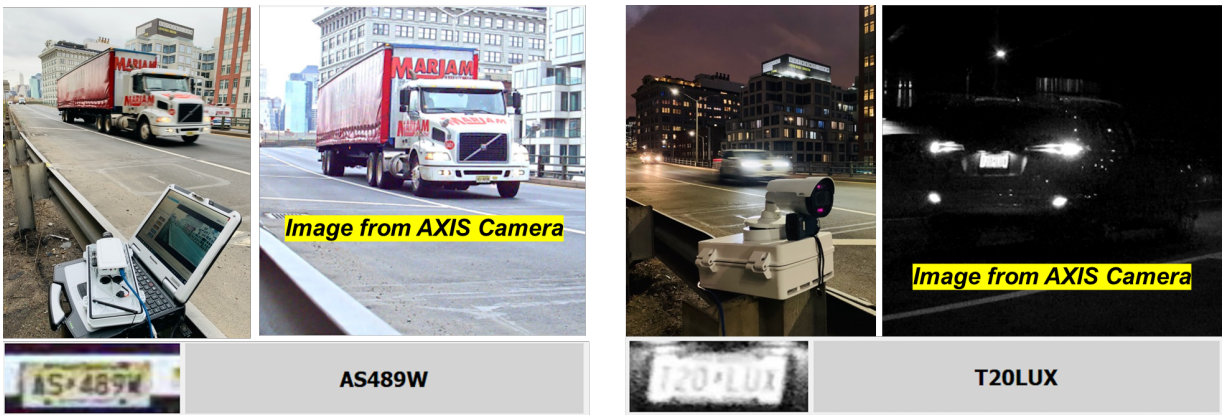

Figure 7 – Evaluation of SW-based ALPR System using non-proprietary AXIS cameras

Other technologies are also reviewed to integrate with the A-WIM system, such as the radio frequency identification (RFID) system. A passive RFID tag can store different truck information, such as permit number, permit period, axle weight and spacing configuration, etc. If the RFID tag and USDOT truck number can be linked with the WIM data, the A-WIM system could provide additional information on the overweight truck, whether it has been issued a permit, and if so, whether it complies with its permit record.

2.3. Implementation of Structural Health Monitoring System in New Smart Roadway Testbed

In addition to the implemented A-WIM system, a Structural Health Monitoring (SHM) system has also been launched on the BQE in the summer of 2021. The SHM system was utilized to evaluate structural responses as well as correlate with the truck statistics from the A-WIM system to provide a comprehensive study of the impact of overweight trucks on major infrastructure.

The sensors were placed at the specific spans for both Staten Island bound (SIB) and Queens bound (QB) to provide insight into the structure's behavior under the traffic loading. Span 18 and Span 6 were selected to monitor their behavior in SIB direction and QB direction, respectively. Various sensors

including accelerometers, tiltmeters, and strain transducers, were installed on these two spans and two adjacent spans in each direction. The SIB Span 18 (SIB-18) was chosen as a case of severe structural condition, and the QB Span 6 (QB6) was selected as a case of good structural condition. Figure 8 and Figure 9 summarize the sensors' locations for Staten Island Bound (SIB) and Queens Bound (QB), respectively. The grey shape on the left side of each figure represents the cross-section of the BQE in each direction.

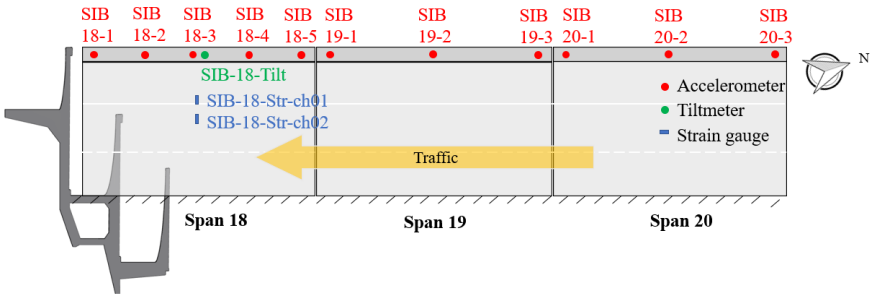

Figure 8 – SIB Sensor Configuration.

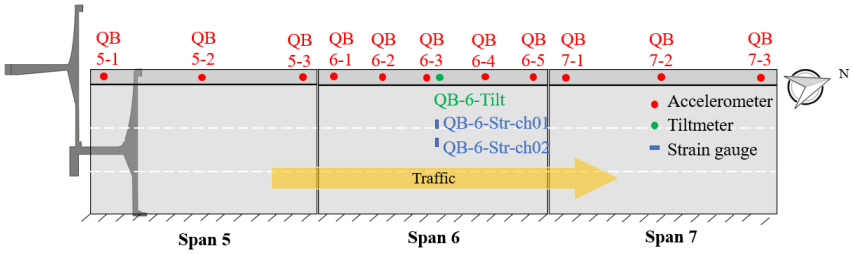

Figure 9 – Initial QB Sensor Configuration.

After a while, the monitored spans for QB were expanded from 3 spans to 9 spans, covering Span 2 to Span 10. Span 6 was still the center of the monitoring because it was found from the previous analysis that the midspan of Span 6 has the largest vibration under the traffic. The new sensor configuration is revised as Figure 10.

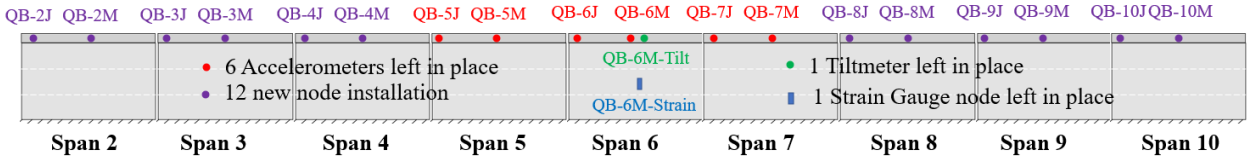

Figure 10 – New QB Sensor Configuration.

2.2. Correlation of SHM and WIM Data

The traffic on QB can be clearly observed from the promenade, whereas the traffic on SIB is hard to be observed from any reachable locations. In addition, at SIB, the cantilever section is designated as a shoulder lane and does not carry regular traffic. Therefore, the correlation of SHM and WIM data was conducted for QB only.

Hourly-Basis Correlation

Among the locations being monitored, the midspan of Span 6 has been observed to have the most critical acceleration in terms of both the number of events and the acceleration magnitude. Therefore, to show the time-dependent trend of the cantilever vibration, QB-6-3 data were used. Figure 11(a) and Figure 11(b) show that the hourly number of events and the hourly maximum acceleration recorded in QB-6-3 node per day are greater during 11 PM and 7 AM, respectively, in which the "event" is captured when the cantilever acceleration exceeds 0.2g, set threshold, under the traffic loading. Bi-weekly data were used. It is observed that the events are more likely to be triggered during midnight time.

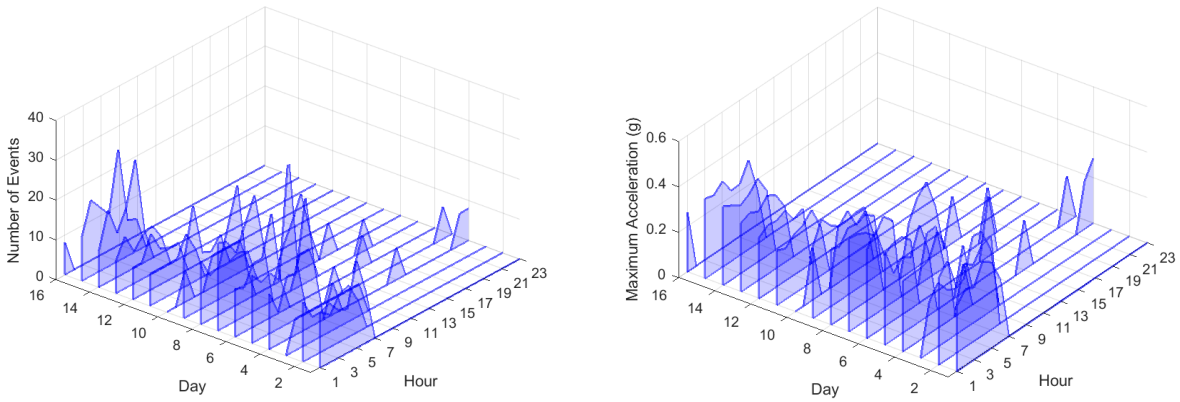

(a) Hourly number of events per day

(b) Hourly maximum acceleration per day

Figure 11 – SHM hourly-basis analysis

This phenomenon is found to correlate with truck traffic. To further understand the correlation between the SHM data and the truck traffic data, an hourly-basis analysis regarding the truck gross vehicle weight (GVW) and speed was performed. WIM data collected by the Kistler system were used to evaluate the truck traffic features as it was proved to be better calibrated. The WIM data collected from the same period as the SHM data were analyzed. Figure 12(a) shows that the hourly mean GVW was higher between 9 PM and 8 AM, except when the research team had the stop-and-go test. During weekdays,

Figure 12(b) shows that the hourly mean speed was higher between 11 PM and 6 AM. The average speed observed on weekends tends to be more constant throughout the day on Saturday. By comparing the hourly variation between SHM and WIM data, it was found that the cantilever vibration is, on the one hand, positively correlated with the truck GVW. On the other hand, the higher acceleration in the nighttime results from the higher truck speed during the nighttime. Due to the change in lane configuration at Joralemon St. (from 3 lanes to 2 lanes), severe congestion is observed during the daytime, resulting in low vibrations.

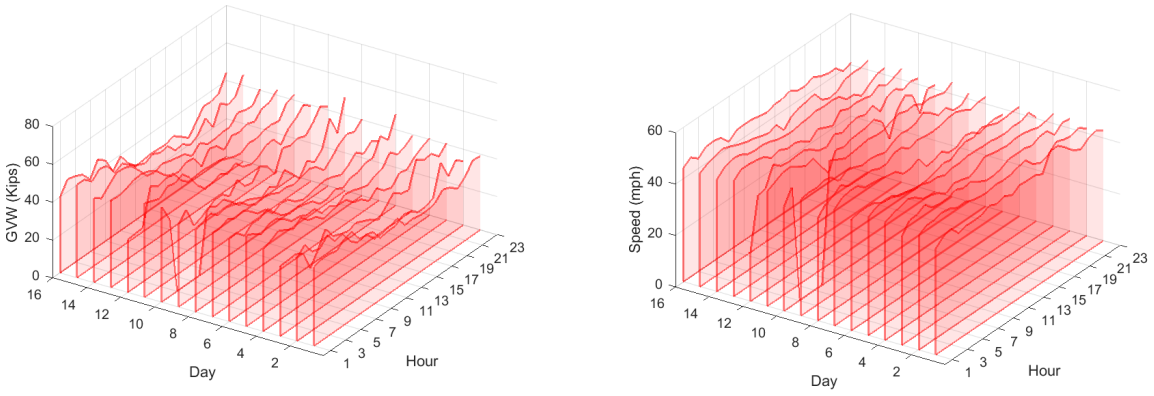

(a) Hourly mean GVW per day

(b) Hourly mean speed per day

Figure 12 –WIM hourly-basis analysis.

To further investigate the correlation between SHM and WIM data, burst data samples were also collected on nodes QB-5M, QB-6M and QB-7M. Burst data is collected by sensors once every preset period. The samples were recorded for 15 seconds every 15 minutes, e.g., four burst data samples were collected every hour. The mean values of maximum peaks are presented in Figure 13.

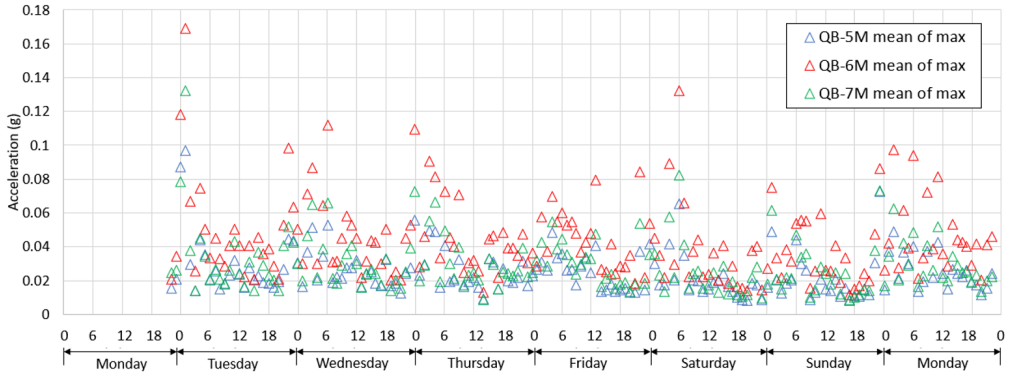

Figure 13 – Summary of the mean of max. acceleration peaks recorded in burst data samples.

For each node, the mean of acceleration peaks and the mean of maximum peaks were correlated to the average gross vehicle weight and the average speed recorded in the Kistler WIM system. The results are presented in Figure 14 to Figure 16.

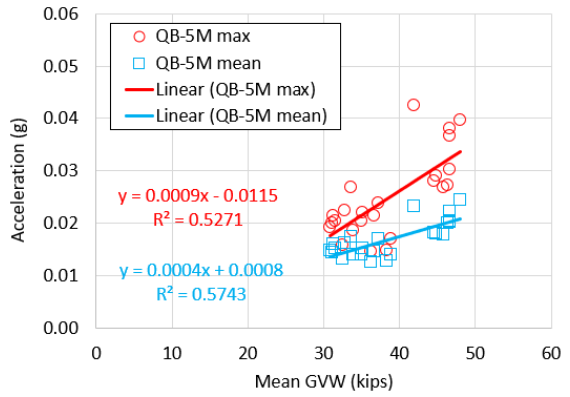

(a) Acceleration vs. Mean GVW

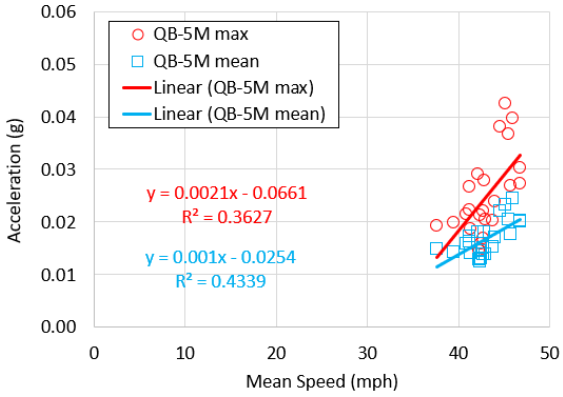

(b) Acceleration vs. Mean Speed

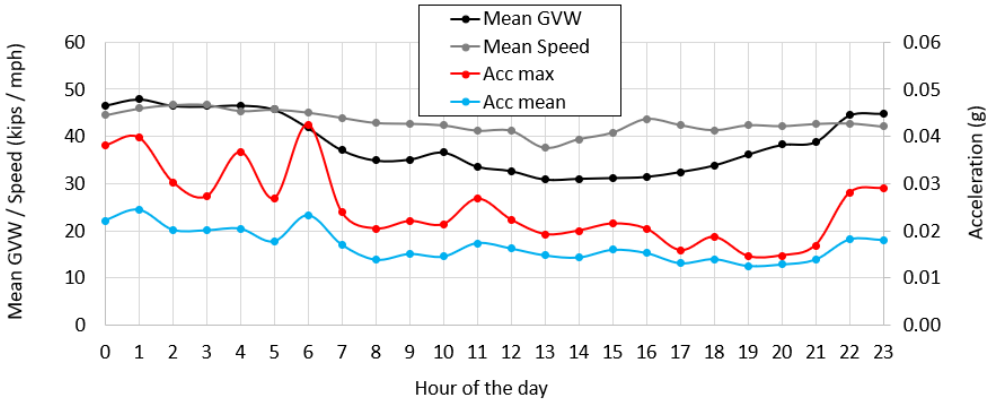

(c) Hourly trend

Figure 14 – Correlation of SHM and WIM considering node QB-5M.

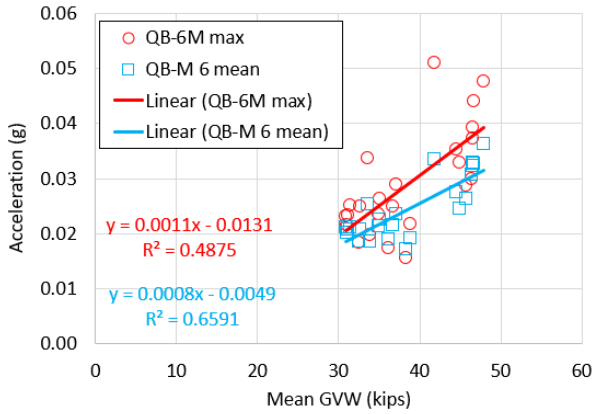

(a) Acceleration vs. Mean GVW

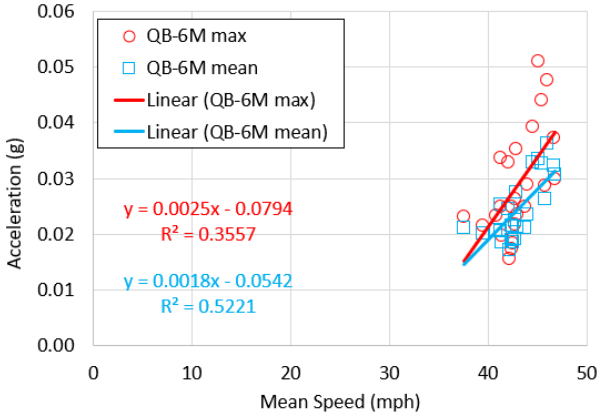

(b) Acceleration vs. Mean Speed

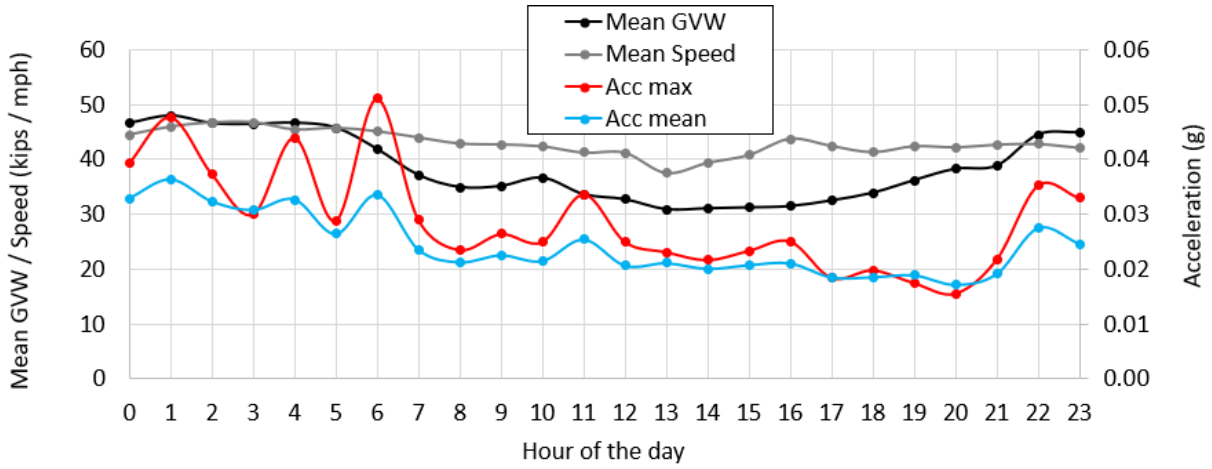

(c) Hourly trend

Figure 15 – Correlation of SHM and WIM considering node QB-6M.

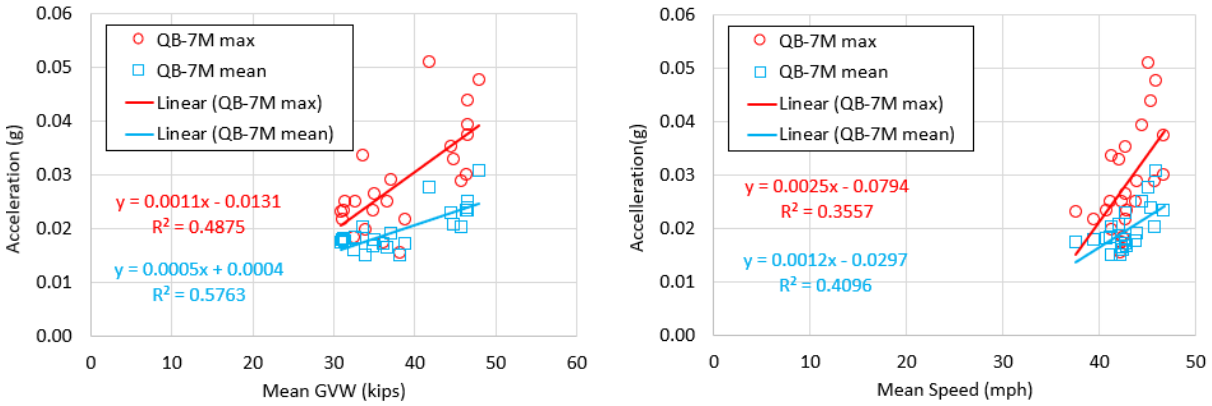

(a) Acceleration vs. Mean GVW

(b) Acceleration vs. Mean Speed

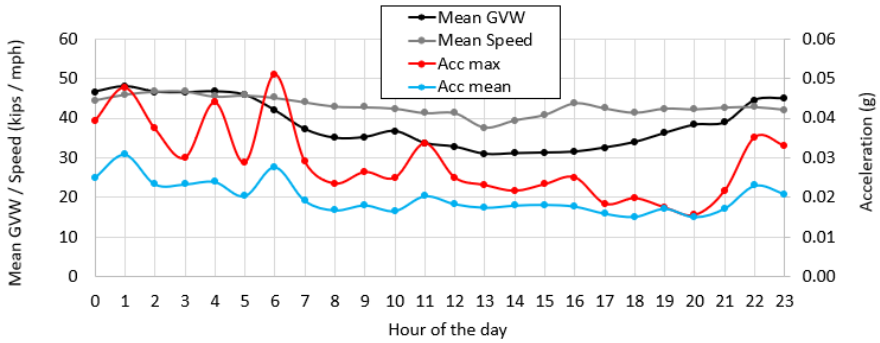

(c) Hourly trend

Figure 16 – Correlation of SHM and WIM considering node QB-7M.

For all cases, the hourly-basis results show that the acceleration data is well correlated to truck GVW and speed. However, it is worth noting that the WIM station is located 1 mile away from the monitored cantilever segments, and the traffic jam at the WIM station is less intense than at the SHM station. Therefore, the traffic speed at the WIM station is expected to be higher than the speed at the bridge.

Correlation of Individual Truck Events

In addition to the hourly-basis correlation, a one-on-one correlation of individual truck events was performed to further confirm the relationship between truck traffic and bridge responses. In the correlation of individual truck events, the same trucks that pass the SHM and WIM stations were identified from the traffic fleet, and their resulting bridge responses were compared to their weight and speed. To perform such an analysis, the research team was grouped into two crews. One crew stayed at the SHM station, and another crew stayed at the WIM station. Once the calibration test began, real time SHM and WIM data were collected, while the videos at two sites were also recorded.

Two calibration tests performed allow the one-on-one correlation analysis. The first calibration test was done, and the strain response of the cantilever deck was of interest. Two crews at WIM and SHM sites focused on Class 9 vehicles (5-axle trucks) and identified the same trucks that passed thru both sites. Figure 17 summarizes all the correlations between cantilever deck responses to the truck weight. Since Class 9 trucks generally have a long wheelbase that is about the same span length as the cantilever segments, a single span might be impacted by the tandem loads rather than the gross vehicle weights. Therefore, Figure 17 depicts the strain response to both GVW and tandem loads. It is observed that truck weight is positively correlated with the deck strain response with high R^2.

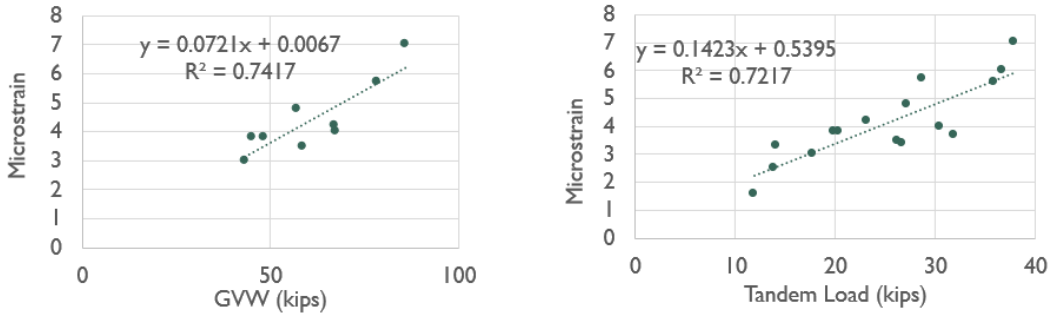

Figure 17 – Correlation between Strain and GVW / Tandem Weights.

The team performed another calibration test to further investigate whether WIM data would be comparable with the acceleration measurements. The test was performed after midnight to capture the speed variance when there was no congestion on the monitored QB spans. Since matching the GVW from WIM data with the acceleration peaks recorded in the bridge was challenging, the following algorithm was used (Figure 18).

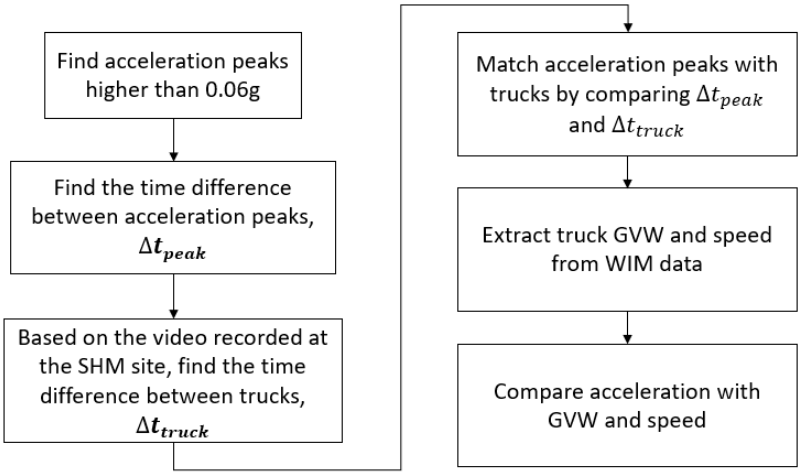

Figure 18 – Algorithm to correlate WIM data with acceleration data.

The threshold of 0.06g was defined to identify the acceleration peaks aiming to capture a larger range of GVW. Thus, twenty acceleration peaks were identified. Figure 19 shows the recorded acceleration data and the identified peaks at QB-6M and Figure 20 presents the summary of results.

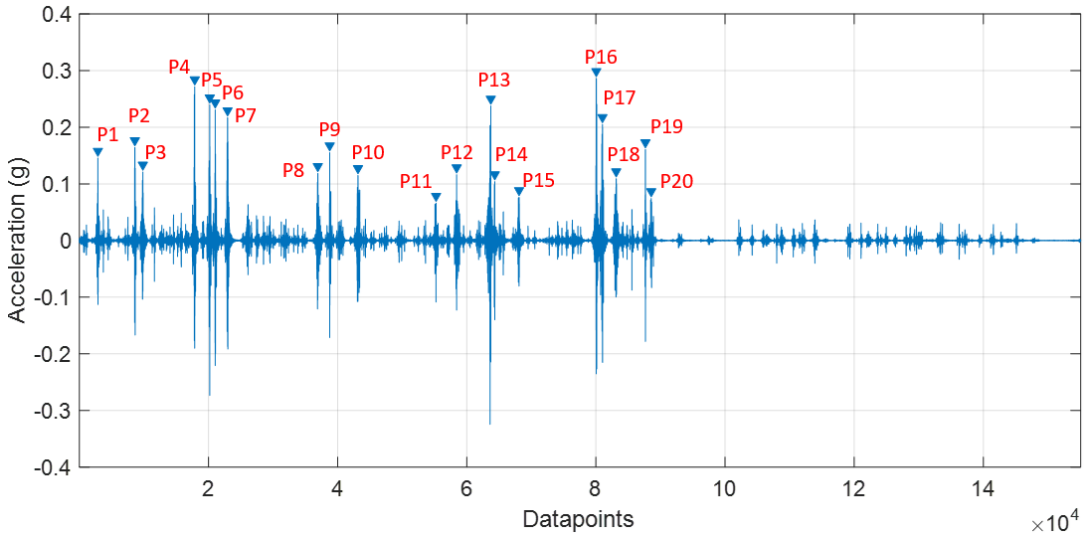

Figure 19 – Identification of acceleration peaks.

The plots presented in Figure 20 consider the trucks running on the left lane (close to the cantilever tip) only. Moreover, since this test was performed under no traffic conditions, it is assumed that the truck speed at the SHM site is the same at the WIM site.

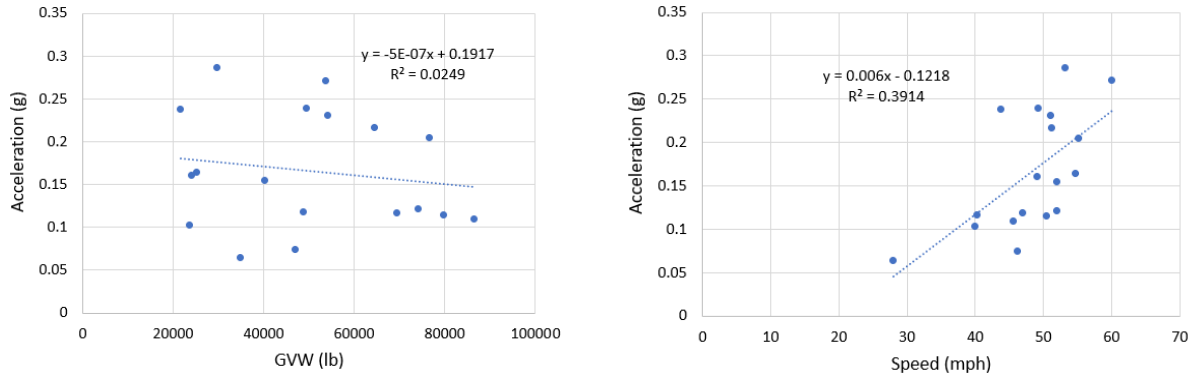

(a) Acceleration vs. GVW (b) Acceleration vs. Speed

Figure 20 – Correlation of acceleration with WIM data (QB-6M).

Section 3 – Evaluation of Smart Roadway Testbed

This section discusses the evaluation of smart roadway testbed in two aspects. The comparisons of measurements of GVW data provided by Kistler and IRD systems are firstly investigated. Then the integration of WIM data and ALPR data is presented.

3.1. Comparison of GVW measurements from Kistler and IRD

Random truck traffic

The gross vehicle weight (GVW) of the random truck traffic population was compared among the measurements provided by both the piezoquartz sensors (Kistler system) and the piezopolymer sensors (IRD system) on the QB I-278 middle lane. The data from May 2022 was used in this analysis.

The timestamp from each vehicle was used as the criteria to match Kistler and IRD records. For this purpose, a variable called “time ID” was created to convert the date and time information from each measurement into seconds units. The Kistler “time ID” variable was added by 80 seconds to account for the clock differences between both systems.

The GVW comparison for each truck classification, e.g., class 5 to class 11 according to FHWA, is depicted in Figure 21. Both, one-to-one comparison as well as the histogram obtained from each weigh-in-motion system is presented. There was no data for truck class 12 and 13, thus the results were not presented.

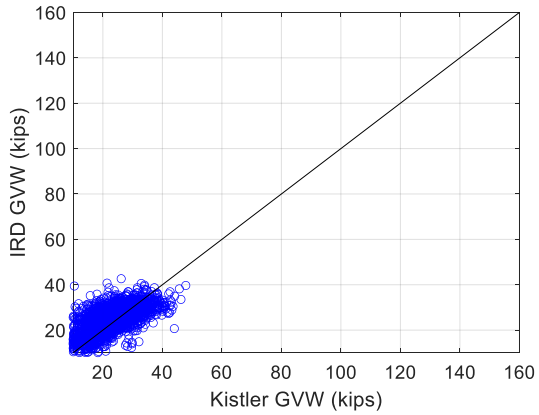

(a) Class 5: one-to-one GVW comparison

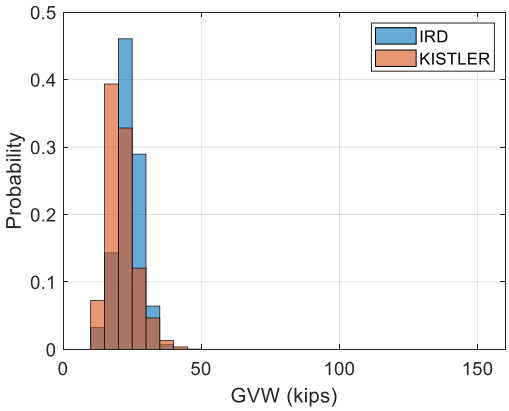

(b) Class 5: GVW histogram

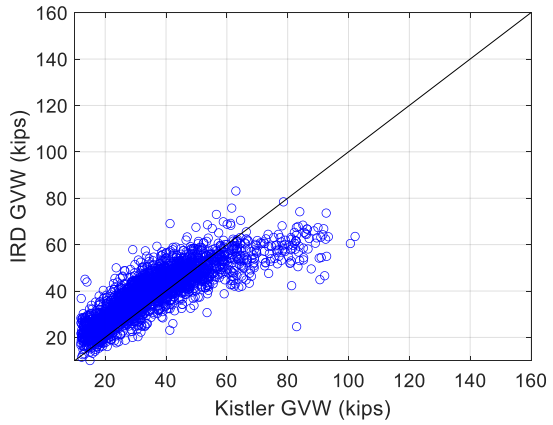

(c) Class 6: one-to-one GVW comparison

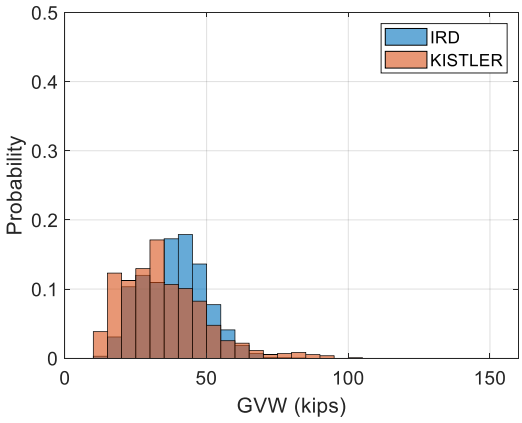

(d) Class 6: GVW histogram

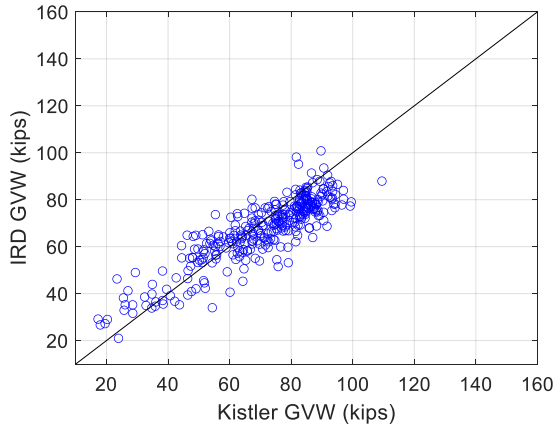

(e) Class 7: one-to-one GVW comparison

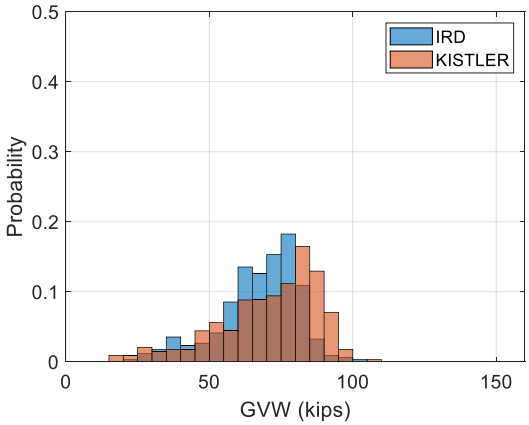

(f) Class 7: GVW histogram

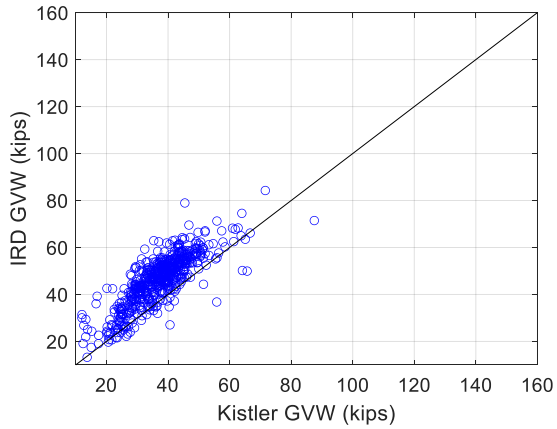

(g) Class 8: one-to-one GVW comparison

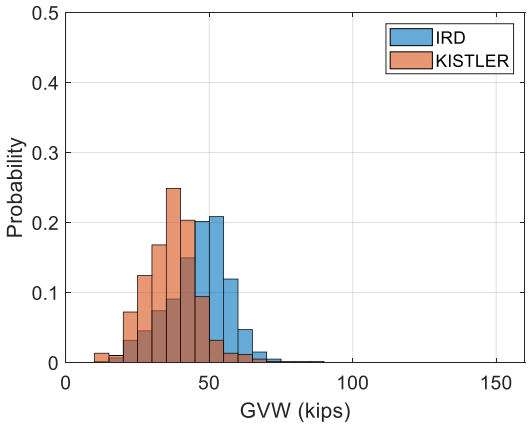

(h) Class 8: histogram

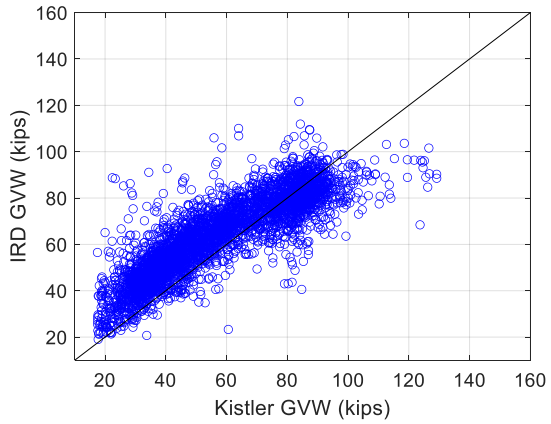

(i) Class 9: one-to-one GVW comparison

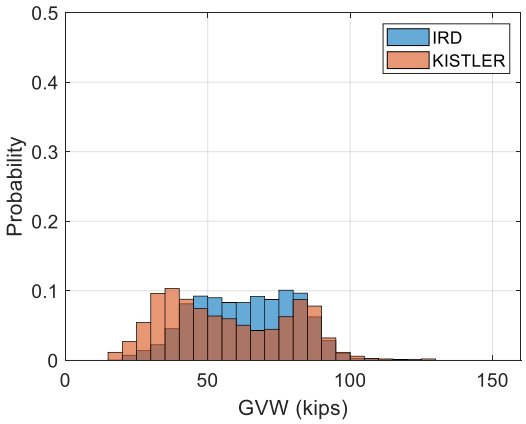

(j) Class 9: histogram

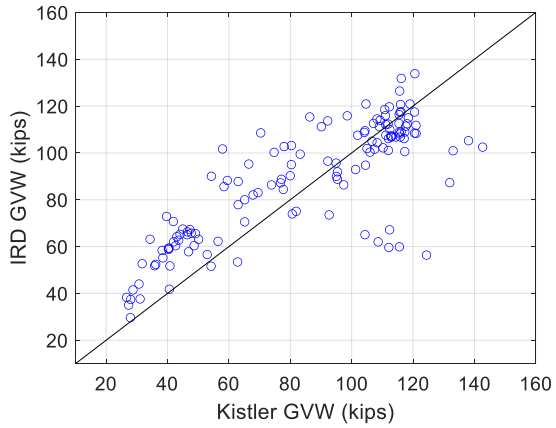

(k) Class 10: one-to-one GVW comparison

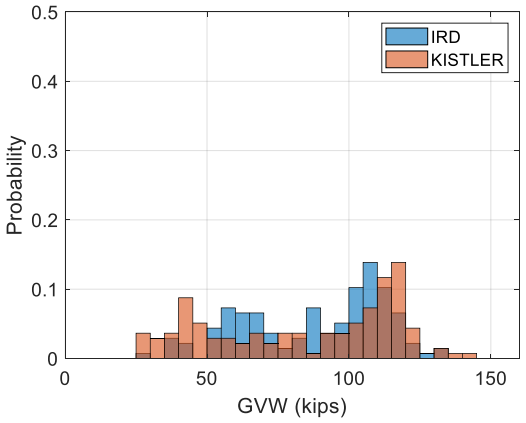

(l) Class 10: histogram

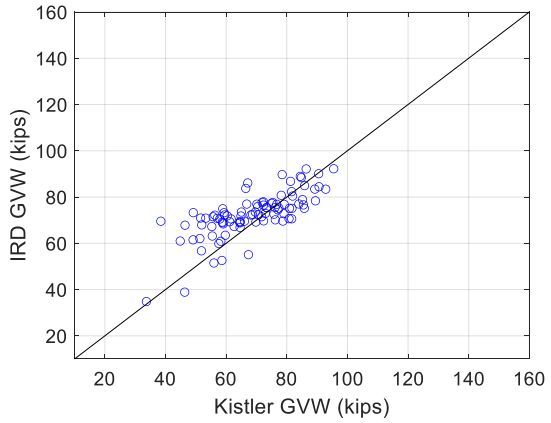

(m) Class 11: one-to-one GVW comparison

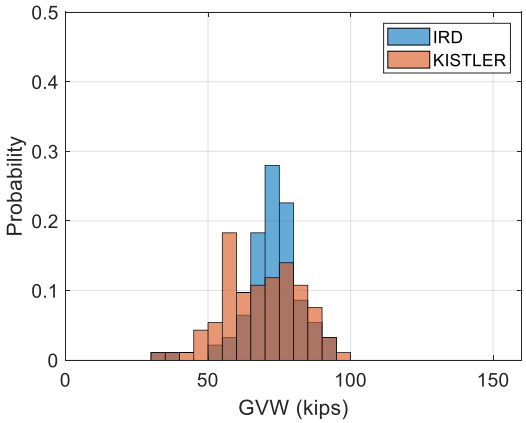

(n) Class 11: histogram

Figure 21 – Gross vehicle weight comparison among Kistler and IRD WIM systems.

From the one-to-one comparison plots, it is observed that most of the data points fall above the line of equality (forty-five-degree line), indicating that the IRD system tends to overestimate GVW in comparison to the Kistler system. This observation can also be confirmed based on the gross vehicle weight histograms in which IRD depicts higher mean values than Kistler. One exception was found for Class 7 trucks, where both the one-to-one plot and the histogram show that the IRD GVW records tend to be less than the Kistler system.

The overall findings discussed above can be confirmed by the error plot in the normal probability paper. Since the Kistler is assumed to be the more accurate system due to its sensor technology, the IRD error is calculated according to Equation 1. The error plot is depicted in Figure 22. It is observed that Class 7 has the only negative mean error, e.g., - 5.6%. The IRD error statistic is summarized in Table 1.

$$IRD\ error\ (\%) = \left(\frac{GVW_{IRD}}{GVW_{Kistler}} - 1\right) \times 100 \qquad (Equation\ 1)$$

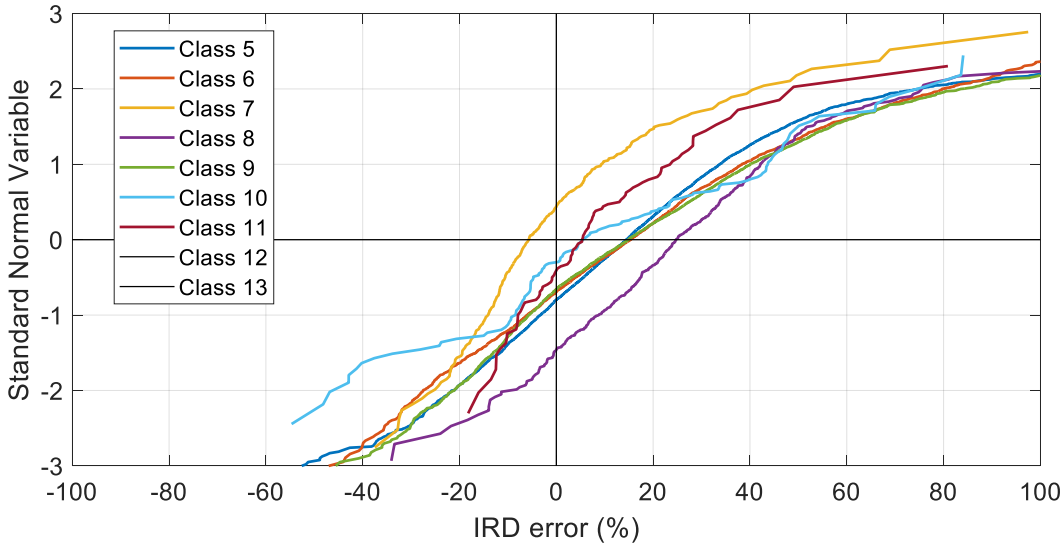

Figure 22 – IRD error plot in normal probability paper.

Table 1. IRD error statistics per truck classification.

Class	IRD mean error (%)	IRD standard deviation error (%)
5	17.1	27.2
6	17.1	25.8
7	-2.4	15.8
8	26.7	21.0
9	18.4	27.5
10	11.6	27.7
11	7.7	16.0

The highest mean error occurs in Class 8 whereas the Class 9 has a higher dispersion of errors than the other cases. It is notable from the one-to-one GVW plots for classes 6 to 9 that the IRD GVW measurements below 60 kips is overestimated and beyond it is underestimated. Therefore, it would be more realistic to extract the error statistic within certain GVW ranges.

3.2. Practice of Autonomous Enforcement

The team has operated both A-WIM and ALPR systems to test an autonomous enforcement tool that integrates both WIM and ALPR systems and other technologies. As both A-WIM and ALPR systems are operating independently, two databases will be maintained. The team focused on identifying and matching all trucks, and legal weight violators (e.g., one or more violation(s) of the gross vehicle weight, single axle weight, tandem or tridem axle weight, and federal bridge formula) to their corresponding license plate and appearance information. For the OW trucks, the team matched two databases based

on the synchronized timestamps and preceding and following vehicles. Figure 23 describes the proposed schematic diagram to synchronize two databases. The integrated system combined two distinct databases of truck weights and configuration information and truck license plate and appearance information. Based on the lessons learned and experiences from this pilot study on the current testbed, the team improved the autonomous enforcement tool and databases.

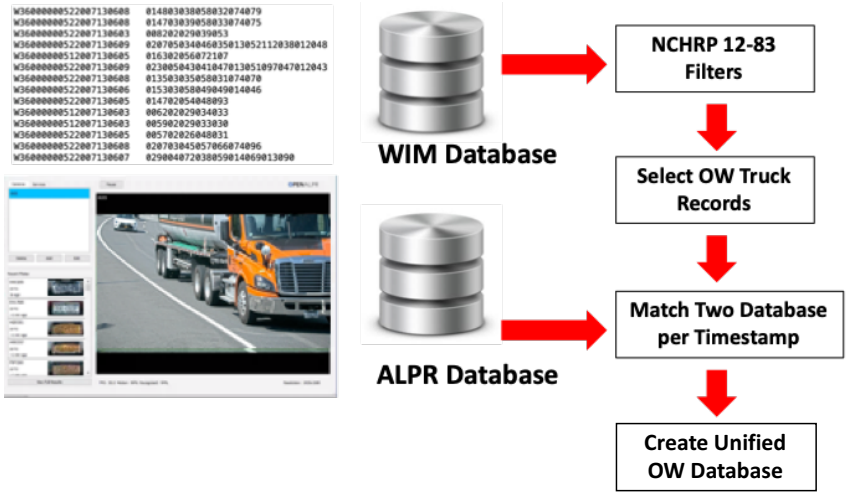

Figure 23 – Schematic Diagram to Integrate and Synchronize WIM and ALPR Database

This section presents the integration of both WIM and ALPR database. Truck records from the WIM system and ALPR system are matched to create the integrated database. Firstly, the integrated data for all truck data is investigated. Then the records of overweight trucks

Integrated Data for all Trucks

One hour of daytime data is used to evaluate the integrated data. Table 2 and Figure 24 summarize the Truck counts for each category during the daytime at 12:20 p.m. till 13:32 p.m. The truck would be identified from the WIM data using the following criteria:

- GVW more than 12 kips
- First axle weight more than 6 kips
- Vehicle length more than 7 ft
- FHWA Class between 3-13

At the first glance, the overall success rate was only 70.9%. However, when vehicles without license plates and vehicles with no plates captured by the ALPR are removed, the success rate is 89.0%. Although the plate reading has not yet been fully checked, the reasons for some of the possible false reading has been found. More discussions could be found in “ALPR Reading Accuracy” section below.

Table 2. Summary of Auto Match for 1hour daytime data

Category	Remarks	Count	Raito 1	Ratio 2
Total WIM		223		
-Invalid WIM	Kistler warning: single track	6		
-Valid WIM	Warning Removed	217	100%	
> No Plate/Not captured	Inherent issue, Not included in success rate	44	20.2%	
> Total Valid Cases	Use for success rate	173	79.7%	
* Success		154	**70.9% (=154/217)**	**89.0% (=154/173)**
* Missed	See **"Missed Cases"** Section for Detail	19	8.7%	10.9%

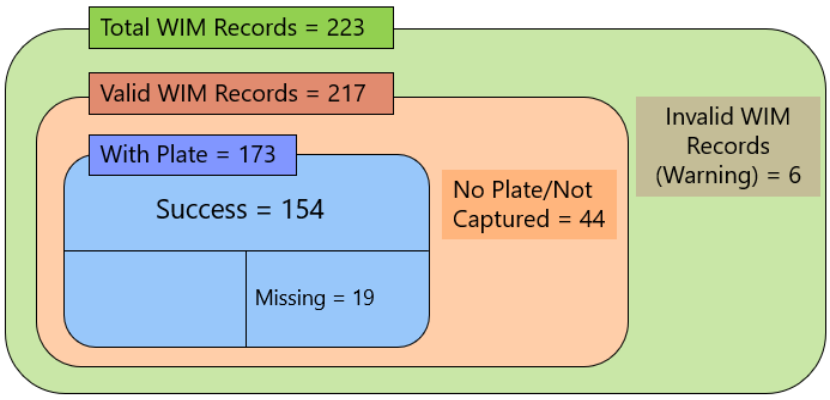

Figure 24 – Diagram for Auto Match for 1hr daytime data for Trucks only (12:20 p.m. to 13:32 p.m.)

Integrated Data for all Overweight Trucks

Table 3 and Figure 25 summarize the overweight truck counts for each category during the daytime at 12:20 p.m. till 13:32 p.m. The overweight trucks are identified from WIM data using the following criteria:

- GVW more than 80 kips or any axle Weight is more than 20000
- First axle weight more than 6 kips
- Vehicle length more than 7 ft
- FHWA Class between 3-13

Similarly, the overall success rate was 62.8%. However, when vehicles without license plates and plates did not capture by the ALPR removed, the success rate would reach 90.0%.

Table 3. Summary of Auto Match for 1hour daytime data for overweight trucks (GVW > 80 kips) only (12:20 p.m. to 13:32 p.m.)

Category	Remarks	Count	Raito 1	Ratio 2
Valid WIM	Warning Removed	43	100%	
> No Plate/Not captured	Inherent issue, Not included in success rate	13	30.2%	
> Total Valid Cases	Use for success rate	30	69.8%	
* Success		27	**62.8% (=27/43)**	**90.0% (=27/30)**
* Missed	See "**Missed Cases**" Section for Detail	3	6.9%	10.0%

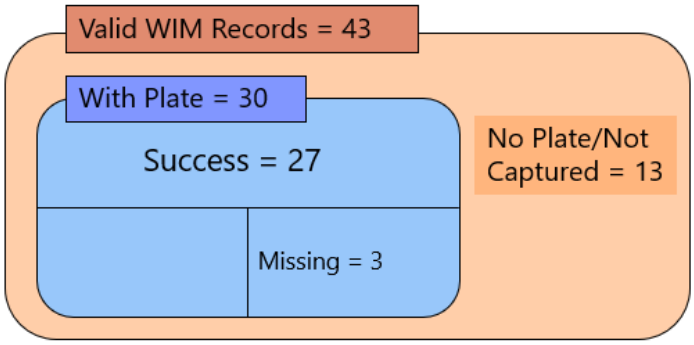

Figure 25 – Diagram for Auto Match for 1hr daytime data for overweight trucks (GVW > 80 kips) (12:20 p.m. to 13:32 p.m.)

ALPR Reading Accuracy

This section evaluates the accuracy of ALPR readings by identifying the reasons of false readings from ALPR as well as the reasons of missed matches. Though the performance of ALPR still requires further testing, some of the cases have been found to cause a false reading by ALPR:

- Lane change: when vehicle shift in or out the lane where ALPR is capturing, the result can be either a wrong plate reading or no reading (miss) at all.
- Other text on the vehicle: when there is other text presented on the front of the vehicle, the ALPR will capture the text instead of the vehicles' plate. In some cases, it may capture both. E.g SCHOOL BUS, UHAUL
- Night performance: ALPR currently has the worse performance in the dark environment resulting in missing plates.

The missed match cases is defined as when there are both WIM records and valid ALPR records for the vehicle, the match algorithm is not able to correctly match both records together by their timestamp. The identified reasons missed match cases are:

- Previous WIM record is not a valid record within a short time, and this causes the matching algorithm to match the ALPR record to the previous WIM record.
- ALPR vehicle time stamp is behind the WIM record's time stamp. The current matching algorithm is programmed so that the ALPR system is ahead of the WIM system. When a vehicle approaches, the ALPR will capture the vehicle first. Thus, in cases when ALPR time stamp is later than the WIM time stamp, the WIM record will be marked as plate not found (Miss).

Table 4, Table 5, Figure 26, and Figure 27 summarized the reason that caused the "Miss" when running 1hr Truck and Overweight vehicle matching.

Table 4. Summary of Missed Cases for 1hour daytime data for Trucks (12:20 p.m. to 13:32 p.m.)

Total Missed Cases	19	100%
Miss caused by record's ALPR time after WIM time	17	89.5%
Miss caused by invalid WIM records within short time	2	10.5%

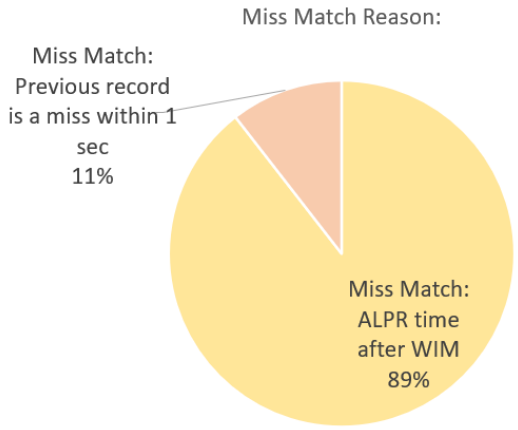

Figure 26 – Diagram for Missed Cases for 1hour daytime data for Trucks (12:20 p.m. to 13:32 p.m.)

Table 5. Summary of Missed Cases for 1hour daytime data for Overweight vehicle (12:20 p.m. to 13:32 p.m.)

Total Missed Cases	3	100%
Miss caused by record's ALPR time after WIM time	2	66.7%
Miss caused by invalid WIM records within short time	1	33.3%

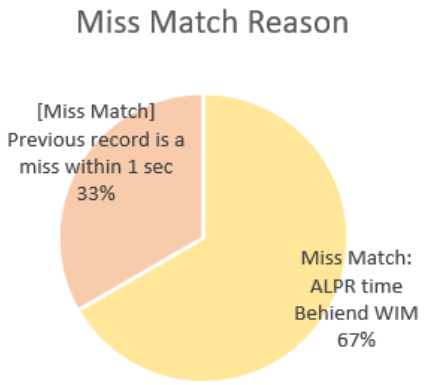

Figure 27 – Diagram for Missed Cases for 1hour daytime data for Overweight vehicle (12:20 p.m. to 13:32 p.m.)

Section 4 – Evaluation of the Impact of OW Truck Enforcement on Load Rating and Reliability Assessment of the Structure

The research team also evaluate the impact of overweight trucks on the load rating and reliability assessment of the structure. The probabilistic live load demand, represented by the live load bias ratio, is derived, and compared to the national live load demand. This section first derives the live load bias ratio for reliability analysis, and then site-specific live load factors are developed for reliability-based load rating method, LRFR.

The NYCDOT plans to implement autonomous enforcement of OW trucks or other types of OW enforcement at the smart roadway testbed to extend the service life of the existing BQE triple cantilever structure. To extend the service life of the BQE structure, adequate law enforcement could be implemented to restrict OW trucks and therefore decrease the impact of live load on the deteriorating concrete sections. It is crucial to understand how the OW enforcement could impact the service life and reliability index of the deteriorated triple cantilever structure carrying the BQE highway. Based on the WIM data collected from the BQE smart roadway testbed, the team determined the average daily traffic (ADT), average daily truck traffic (ADTT), average daily OW truck (OW_ADTT), truck ratio (ADTT/ADT), and OW truck ratio (OW_ADTT/ADTT) over the time. The number of trucks and OW trucks as well as their frequency and OW threshold is the key information to perform the analysis of the extrapolated live load bias ratios. The extrapolated live load bias ratio represents the live load demand in a return period of 5 years (i.e., typical for load rating of bridges), and the team implemented different extrapolation techniques to predict the maximum live load for the return period. The team investigated this impact by the following steps for the project:

- Step 1: Discuss with NYCDOT about the detailed plan for the OW enforcement and its legislation
- Step 2: Obtain the detailed OW violated truck information from the NYCDOT (if available, OW ticket information)
- Step 3: Utilize the machine learning technique to identify the ticketed trucks from the WIM data.
- Step 4: Simulate the truck traffic on BQE under different levels of OW enforcement based on the information from Step 1 to Step 3.
- Step 5: Extrapolate the live load bias ratio based on the OW truck traffic scenarios obtained from Step 4.

4.1. Procedures to Obtain the Live Load Bias Ratio and Live Load Factors

HL93 Live Load Bias Ratio for Reliability Analysis

The WIM data used in the following analysis are based on the truck weight spectra obtained from the piezoelectric sensors. The data period is October 2019 to May 2022 for Queen's bound and October 2019 to December 2020 for Staten Island bound. Based on the AASHTO LRFR recommendations and site-specific Weigh-In-Motion (WIM) data from BQE (AASHTO MBE 2020):

a. Filter the site-specific raw WIM data to exclude erroneous readings and car data (Use NCHRP 12-83 (2014) specified filters).
b. Calculate the load effect ratio of each truck in WIM data based on simply supported span and normalize it by the load effects caused by the HL93 design loads.
c. Sort the ratios and obtain the top 5% upper tail of the load effect ratios
d. Extrapolate the distribution of these load effect ratios for different return periods based on the AASHTO MBE 3rd Edition (LRFR) to get the L_{max}/L_{HL93}.

Live Load Factors for HL93 Load

The procedures to obtain the live load factors for HL93 loading are summarized below. For two-lane loading, the assumption of side-by-side statistics is taken from the AASHTO LRFD (AASHTO LRFD 2020) which are also taken to be similar during the development of the LRFR. The two assumptions are as follows: 1) side by side events occur every 30 trucks, and 2) heavy trucks occur every 15 trucks.

a. Obtain the national average lane load bias ratios that were applied in obtaining the live load factors of AASHTO LRFR, in the case of ADTT=5,000 (Wassef et al. 2014). The maximum value from all spans is used in this study.
    1) For the single-lane load effect, at the 5-year level (i.e., operating), the HL93 bias ratios for live load moment and reaction are **1.41**, and **1.58**, respectively. At the 75-year level (i.e., Inventory), the bias ratios for live load moment and reaction are **1.46**, and **1.63**, respectively.
    2) For the two-lane load effect, at the 5-year level (i.e., operating), NCHRP 12-83 does not provide this data. However, based on BQE data, it was found the maximum trucks side-by-side in two-lane loading is about 82% of the maximum truck in single-lane loading (see Table 8 and Table 9). Therefore, at the 5-year level (i.e., operating), the two-lane bias ratios can be calculated based on the single-lane bias ratios. The bias ratios for live load moment and reaction are **1.16**, and **1.30**, respectively. At the 75-year level (i.e., Inventory), the AASHTO LRFD mentions the trucks in two-lane loading are equivalent to the two-month maximum truck in single-lane loading. The bias ratios for live load moment and reaction are taken from Table 6 and Table 7 as **1.34**, and **1.48**, respectively.

Table 6. National bias ratio for live load moment (Wassef et al. 2014)

Table 4-8 Statistical Parameters of Live Load Moments for ADTT 5,000, $\lambda = \mu + 1.5\sigma$

	ADTT 5,000																	
Span	30 ft			60 ft			90 ft			120 ft			200 ft			300 ft		
	λ	μ	COV	λ	μ	COV	λ	μ	COV	λ	μ	COV	λ	μ	COV	λ	μ	COV
1 Day	1.08	0.85	0.18	1.02	0.82	0.17	1.03	0.82	0.17	1.03	0.82	0.17	0.95	0.75	0.17	0.84	0.67	0.17
2 Weeks	1.24	0.98	0.17	1.26	1.00	0.17	1.24	1.00	0.16	1.24	1.04	0.13	1.16	0.96	0.14	1.06	0.88	0.14
1 Month	1.28	1.04	0.15	1.32	1.03	0.18	1.30	1.12	0.11	1.26	1.11	0.09	1.20	0.99	0.14	1.13	0.93	0.14
2 Months	1.31	1.07	0.15	1.34	1.07	0.17	1.32	1.15	0.10	1.31	1.14	0.10	1.23	1.02	0.14	1.16	0.96	0.14
6 Months	1.34	1.11	0.14	1.35	1.11	0.14	1.34	1.19	0.08	1.32	1.17	0.09	1.28	1.04	0.15	1.23	1.00	0.15
1 Year	1.35	1.14	0.12	1.38	1.14	0.14	1.38	1.21	0.09	1.36	1.19	0.09	1.31	1.07	0.15	1.25	1.02	0.15
5 Years	1.39	1.16	0.13	1.40	1.19	0.12	1.40	1.25	0.08	1.41	1.21	0.11	1.34	1.10	0.15	1.28	1.05	0.15
50 Years	1.41	1.21	0.11	1.44	1.24	0.10	1.44	1.27	0.09	1.46	1.23	0.12	1.39	1.13	0.15	1.30	1.06	0.15
75 Years	1.42	1.22	0.11	1.45	1.25	0.10	1.45	1.29	0.08	1.46	1.25	0.11	1.40	1.14	0.15	1.31	1.07	0.15
100 Years	1.42	1.23	0.11	1.45	1.26	0.10	1.47	1.30	0.08	1.47	1.26	0.11	1.40	1.15	0.15	1.33	1.08	0.15

Table 7. National Bias Ratio for Live Load Reaction, Shear (Wassef et al. 2014)

Table 4-13 Statistical Parameters of Live Load Reactions for ADTT 5,000, $\lambda = \mu + 1.5\sigma$

	ADTT 5000																	
Span	30 ft			60 ft			90 ft			120 ft			200 ft			300 ft		
	μ+1.5σ	μ	COV	μ+1.5σ	μ	COV	μ+1.5σ	μ	COV	μ+1.5σ	μ	COV	μ+1.5σ	μ	COV	μ+1.5σ	μ	COV
1 Day	1.25	1.05	0.12	1.09	0.94	0.11	1.14	0.96	0.13	1.12	0.94	0.13	1.02	0.84	0.14	0.90	0.74	0.14
2 Weeks	1.42	1.19	0.13	1.30	1.10	0.12	1.36	1.13	0.13	1.36	1.13	0.13	1.26	1.03	0.15	1.13	0.93	0.15
1 Month	1.46	1.22	0.13	1.34	1.13	0.12	1.39	1.16	0.13	1.40	1.17	0.13	1.30	1.06	0.15	1.18	0.96	0.15
2 Months	1.48	1.24	0.13	1.36	1.15	0.12	1.43	1.20	0.13	1.44	1.20	0.13	1.33	1.09	0.15	1.21	0.99	0.15
6 Months	1.51	1.27	0.13	1.39	1.18	0.12	1.47	1.23	0.13	1.48	1.24	0.13	1.39	1.13	0.15	1.27	1.03	0.15
1 Year	1.54	1.28	0.13	1.41	1.20	0.12	1.50	1.26	0.13	1.51	1.27	0.13	1.41	1.15	0.15	1.29	1.06	0.15
5 Years	1.58	1.32	0.13	1.48	1.25	0.12	1.54	1.30	0.12	1.56	1.30	0.13	1.46	1.19	0.15	1.34	1.09	0.15
50 Years	1.62	1.36	0.13	1.53	1.29	0.12	1.59	1.35	0.12	1.61	1.35	0.13	1.52	1.23	0.15	1.40	1.14	0.15
75 Years	1.63	1.37	0.12	1.54	1.30	0.12	1.60	1.36	0.12	1.62	1.36	0.13	1.53	1.24	0.15	1.41	1.15	0.15
100 Years	1.63	1.38	0.12	1.55	1.31	0.12	1.61	1.37	0.12	1.62	1.37	0.13	1.53	1.25	0.15	1.42	1.15	0.15

Table 8. Bias Ratios in Single-Lane Loading and Two-Lane Loading Based on BQE SIB Data

Return Period	Moment		Shear		Ratio	
	Single-lane max truck (1)	Two-lane max truck (2)	Single-lane max truck (3)	two-lane max truck (4)	(2)/(1)	(4)/(3)
1-Year	1.48	1.12	1.56	1.18	76%	76%

5-Year	1.56	1.23	1.64	1.29	79%	79%
10-Year	1.59	1.27	1.68	1.33	80%	80%
20-Year	1.62	1.31	1.71	1.38	81%	81%
30-Year	1.64	1.33	1.73	1.40	81%	81%
40-Year	1.65	1.35	1.75	1.42	82%	81%
50-Year	1.66	1.36	1.76	1.43	82%	82%
75-Year	1.68	1.38	1.78	1.46	82%	82%
				Governing	**82%**	**82%**

Table 9. Bias Ratios in Single-Lane Loading and Two-Lane Loading Based on BQE QB Data

Return Period	Moment		Shear		Ratio	
	Single-lane max truck (1)	Two-lane max truck (2)	Single-lane max truck (3)	two-lane max truck (4)	(2)/(1)	(4)/(3)
1-Year	1.60	1.22	1.68	1.28	76%	76%
5-Year	1.69	1.33	1.77	1.40	79%	79%
10-Year	1.72	1.38	1.8	1.44	80%	80%
20-Year	1.76	1.42	1.84	1.49	81%	81%

30-Year	1.78	1.45	1.86	1.52	81%	81%
40-Year	1.79	1.47	1.88	1.53	82%	82%
50-Year	1.80	1.48	1.89	1.55	82%	82%
75-Year	1.82	1.50	1.91	1.57	83%	82%
				Governing	**83%**	**82%**

b. Adjustment of the live load factors based on bias ratios from WIM data:

$$\gamma_{LL}(\text{adjusted, single lane}) = \left(\frac{\text{Maximum single lane load effect (WIM Truck Data)} * \text{GDF}_{one}}{\text{Maximum single lane load effect (LRFR Truck Data)} * \text{GDF}_{one}}\right) \gamma_{LL}(\text{LRFR}) \quad \text{Equation (1)}$$

$$\gamma_{LL}(\text{adjusted, two lane}) = \left(\frac{\text{Maximum two lanes load effect (WIM Truck Data)} * \text{GDF}_{two}}{\text{Maximum two lanes load effect (LRFR Truck Data)} * \text{GDF}_{two}}\right) \gamma_{LL}(\text{LRFR})$$

Equation (2)

Note that Girder Distribution Factors (GDF) are not affecting the results.

c. Adjustment for seasonal variation: the updated live loads are derived from more than two years of WIM data. No seasonal adjustment is needed.

Bias Ratio for Reliability Analysis

Table 10 shows the results for the BQE site-specific HL93 bias ratios from WIM data.

Table 10. Per Lane live load bias ratio from site-specific BQE WIM data (Using HL93)

Return Periods	Single Lane Bias Ratio - Approach I			
	SIB-Moment	SIB-Shear	QB-Moment	QB-Shear
1-Year	1.48	1.56	1.60	1.68
5-Year	1.56	1.64	1.69	1.77
10-Year	1.59	1.68	1.72	1.80
20-Year	1.62	1.71	1.76	1.84
30-Year	1.64	1.73	1.78	1.86
40-Year	1.65	1.75	1.79	1.88
50-Year	1.66	1.76	1.80	1.89
75-Year	1.68	1.78	1.82	1.91

Based on the finite element models of the structure, the ratios of load effects from HL93 loads and Type 3S2 legal load are shown in Table 11. The lane live load bias ratio from the site-specific BQE WIM data could also be represented in the form of Type 3S2 based on the equation below:

$$Bias\ Ratio\left(\frac{Extrapolated\ live\ load\ effect}{live\ load\ effect\ by\ Type\ 3S2}\right) = Bias\ Ratio\left(\frac{Extrapolated\ live\ load\ effect}{live\ load\ effect\ by\ HL93}\right) \times \frac{live\ load\ effect\ by\ HL93}{live\ load\ effect\ by\ Type\ 3S2} \quad \text{Equation (3)}$$

Table 12 shows the results of the lane live load bias ratio from site-specific BQE WIM data using Type 3S2. Since two-lane loading does not control the load rating, only single-lane loading is provided.

Table 11. Load Effect Ratio between HL93 and Type 3S2 legal load (Single Lane)

Load Case Ratio	Section Cut Location	Moment	Shear
HL93/Type 3S2	SCUT1(E2-Begin-7.5)	1.70	1.71
HL93/Type 3S2 - 120K	SCUT1(E2-Begin-7.5)	1.02	1.02

Table 12. Lane live load bias ratio from site-specific BQE WIM data (Using Type 3S2)

Return Periods	**Single Lane Bias Ratio - Approach I**			
	SIB-Moment	SIB-Shear	QB-Moment	QB-Shear
1-Year	2.51	2.66	2.72	2.87
5-Year	2.65	2.81	2.87	3.02
10-Year	2.70	2.87	2.93	3.09
20-Year	2.76	2.93	2.99	3.15
30-Year	2.79	2.96	3.02	3.18
40-Year	2.81	2.98	3.04	3.21
50-Year	2.83	3.00	3.06	2.23
75-Year	2.86	3.04	3.10	3.26

4.2. Recommended Live Load Factors for Load Rating

Recommended Live Load Factors for HL93 Loading

The recommended live load factors for the HL93 load are summarized in Table 13, Table 14, Table 15, and Table 16. Note that the AASHTO MBE (LRFR) specifies live load factors of 1.35 and 1.75 for Operating (equivalent to 5 years) and Inventory (equivalent to 75 years) levels, respectively. For return periods for more than 5 years, the live load factors are given at the inventory level in Table 14 and Table 16.

Table 13. Recommended Live Load Factors, $\gamma_{LL,HL93,Operating}$, for HL93 Load at Operating Level (Beta=2.5), without Multiple Presence Factor

Operating level	**Single-Lane**				**2-Lane**			
Return Period	Moment (SIB)	Shear (SIB)	Moment (QB)	Shear (QB)	Moment (SIB)	Shear (SIB)	Moment (QB)	Shear (QB)
5-Year	1.48	1.40	1.60	1.51	1.43	1.34	1.55	1.45

Table 14. Recommended Live Load Factors, $\gamma_{LL,HL93,Inventory}$, for HL93 Load at Inventory Level (beta=3.5), without Multiple Presence Factor

Inventory level	**Single-Lane**				**2-Lane**			
Return Period	Moment (SIB)	Shear (SIB)	Moment (QB)	Shear (QB)	Moment (SIB)	Shear (SIB)	Moment (QB)	Shear (QB)
10-Year	1.91	1.80	2.07	1.94	1.66	1.58	1.80	1.71

20-Year	1.94	1.84	2.11	1.98	1.71	1.63	1.86	1.76
30-Year	1.97	1.86	2.13	2.00	1.74	1.66	1.89	1.79
40-Year	1.98	1.87	2.15	2.01	1.76	1.68	1.91	1.81
50-Year	1.99	1.89	2.16	2.03	1.78	1.69	1.93	1.83
75 Year	2.02	1.91	2.18	2.05	1.81	1.72	1.96	1.86

Table 15. Recommended Live Load Factors, $\gamma_{LL,HL93,Operating}$, for HL93 Load at Operating Level (Beta=2.5), with Multiple Presence Factor

Operating level	**Single-Lane**				**2-Lane**			
Return Period	Moment (SIB)	Shear (SIB)	Moment (QB)	Shear (QB)	Moment (SIB)	Shear (SIB)	Moment (QB)	Shear (QB)
5-Year	1.77	1.68	1.92	1.81	1.43	1.34	1.55	1.45

Table 16. Recommended Live Load Factors, $\gamma_{LL,HL93,Inventory}$, for HL93 load at Inventory Level (Beta=3.5), with Multiple Presence Factor

Inventory level	Single-Lane				2-Lane			
Return Period	Moment (SIB)	Shear (SIB)	Moment (QB)	Shear (QB)	Moment (SIB)	Shear (SIB)	Moment (QB)	Shear (QB)
10-Year	2.29	2.16	2.48	2.32	1.66	1.58	1.80	1.71
20-Year	2.33	2.21	2.53	2.37	1.71	1.63	1.86	1.76
30-Year	2.36	2.23	2.56	2.40	1.74	1.66	1.89	1.79
40-Year	2.38	2.25	2.58	2.42	1.76	1.68	1.91	1.81
50-Year	2.39	2.26	2.59	2.43	1.78	1.69	1.93	1.83
75 Year	2.42	2.29	2.62	2.46	1.81	1.72	1.96	1.86

Recommended Live Load Factors for AASHTO Type 3S2

RIME converted the live load factors for HL93 to live load factors for Type 3S2 based on the equation below. The results are shown in Table 17 and Table 18. If using AASHTO LRFD GDF equations, Table 17 should be used. If another structural analysis approach is used, e.g., FE model, Table 18 should be used. Since two-lane loading does not control the load rating of the critical section, only live load factors for single-lane loading are provided here. Note that the AASHTO MBE has proposed Equation C6A.4.4.2.3a-6 and C6A.4.4.2.3a-7 (referenced as MBE equations) to calculate the site-specific live load factors for two or more lanes loading case and one lane loading case, respectively. The MBE equations are consistent with Equation (4) when γ_{LL} include the multiple presence factors. The team found out that Equation (4) and the MBE equations produce similar results.

$$\gamma_{LL,3S2} = \left(\frac{\text{Load Effect (HL93)}}{\text{Load Effect (Type 3S2)}}\right)\gamma_{LL,HL93}$$ Equation (4)

Two or more lanes loading case:

$$\gamma_L = \left[\frac{L_{max2}}{LE_2}\right]1.8 > 1.3 \quad \text{(C6A.4.4.2.3a-6)}$$

One lane loading case:

$$\gamma_L = \left[\frac{L_{max1}}{LE_1}\right]1.8 > 1.8 \quad \text{(C6A.4.4.2.3a-7)}$$

where:

L_{max1} = Maximum single-lane load effect expected over a 5-year period

L_{max2} = Maximum two or more lane load effect expected over a 5-year period

LE_1 = Maximum load effect from one 120 K, 3S2 truck

LE_2 = Maximum load effect from two 120 K, 3S2 trucks side by side

Table 17. Recommended Live Load Factors, $\gamma_{LL,Type\ 3S2,Operating}$, for Type 3S2 Load at Operating Level (Beta=2.5), without Multiple Presence Factor

Operating level	Single-Lane				2-Lane			
Return Period	Moment (SIB)	Shear (SIB)	Moment (QB)	Shear (QB)	Moment (SIB)	Shear (SIB)	Moment (QB)	Shear (QB)
5-Year	2.52	2.40	2.73	2.58	2.43	2.29	2.64	2.48

Table 18. Recommended Live Load Factors, $\gamma_{LL,Type\ 3S2,Operating}$, for Type 3S2 Load at Operating Level (Beta=2.5), with Multiple Presence Factor

Operating level	Single-Lane				2-Lane			
Return Period	Moment (SIB)	Shear (SIB)	Moment (SIB)	Shear (SIB)	Moment (SIB)	Shear (SIB)	Moment (SIB)	Shear (SIB)
5-Year	3.02	2.88	3.27	3.10	2.43	2.29	2.64	2.48

Live Load Factors for HS20 Loading.

For the LFR (AASHTO 2002), the specifications do not clearly specify a way to incorporate the effect of the site-specific WIM data. However, the RIME team converted the live load factors from LRFR to LFR and the basis is that under both methods, the live load demand (i.e., the output of the live loading) should remain the same. The live load factors for HS20 loading are based on equating the factored live load in LFR with the factored live load in LRFR as shown in the following equations:

$$\gamma_{LL,HS20} \times \text{Load Effect (HS20)} = \gamma_{LL,HL93} \times \text{Load Effect (HL93)} \qquad \text{Equation (5)}$$

which is re-written as follows:

$$\gamma_{LL,HS20} = \left(\frac{\text{Load Effect (HL93)}}{\text{Load Effect (HS20)}}\right)\gamma_{LL,HL93} \qquad \text{Equation (6)}$$

The ratio $\left(\frac{\text{Load Effect (HL93)}}{\text{Load Effect (HS20)}}\right)$ is based on the results from the JV's FE model analysis for the specific span length (i.e., the ratio is equal to 1.18 for moment and 1.38 for shear). Additionally, the live load statistics and multiple presence factors adopted in LRFD were used in calibrating the live load factors to achieve an average reliability index of 2.5. These statistics include the use of a multiple presence factor equal to 1.20 for single (see Table 19) to emphasize that the probability of a truck in a single lane is heavier than the weight of each truck in two lanes side-by-side is higher.

Table 19. Multiple Presence Factors, m, from AASHTO LRFD (Table 3.6.1.1.2-1)

Number of Loaded Lanes	Multiple Presence Factors, *m*
1	1.20
2	1.00
3	0.85
>3	0.65

Thus, based on the direct conversion of the live load demand from HL93 to HS20 loadings, including all the assumptions made in LRFR for multiple presence factors, Table 22 and Table 23 show the adjusted live load factors at the Operating and Inventory Rating levels for HS20 loading, respectively.

As mentioned earlier, the live loading scenarios for more than one lane, described as "Multiple Presence Effects" in LRFR, and "Reduction in Load Intensity" in LFR, have distinct interpretations in both approaches. In the AASHTO LRFR, the approach specifies that the maximum trucks in single-lane loading, three-lane loading, and more than three-lane loading scenarios are 120%, 85%, and 65% of the maximum truck in two-lane loading scenario, as shown above in Table 19. In the AASHTO LFR, the approach interprets this as "REDUCTION IN LOAD INTENSITY", which specifies 100% for one or two lanes, 90% for three lanes, and 75% for four lanes or more. The difference is that LRFR assumes the maximum truck in one-lane loading is 20% more than the maximum truck in a two-lane loading while the LFR assumes the maximum truck remains the same for both one-lane and two-lane loadings. This would be less conservative for single lane events if the LFR approach is applied literally without converting the LRFR assumptions made for the MPF. Then, the live load factors for the HS20 loading shown in Table 20 and Table 21 for the single lane event are based on the live load demand as formulated in the LRFR. However, the MP effects (i.e., adding a factor of 1.2) were not carried over since the LFR's multiple presence factor is considered 1.0 for one and two lanes.

Table 20. Live Load Factors, $\gamma_{LL,HS20,Operating}$, for HS20 loading at Operating Level without the Multiple Presence Factor

Operating level	**Single-Lane**				**2-Lane**			
Return Period	Moment (SIB)	Shear (SIB)	Moment (QB)	Shear (QB)	Moment (SIB)	Shear (SIB)	Moment (QB)	Shear (QB)
5-Year	1.74	1.94	1.89	2.09	1.68	1.85	1.83	2.11

Table 21. Live Load Factors, $\gamma_{LL,HS20,Inventory}$, for HS20 Loading at Inventory Level without the Multiple Presence Factor

Inventory level	Single-Lane				2-Lane			
Return Period	Moment (SIB)	Shear (SIB)	Moment (QB)	Shear (QB)	Moment (SIB)	Shear (SIB)	Moment (QB)	Shear (QB)
10-Year	2.25	2.49	2.44	2.67	1.96	2.18	2.13	2.36
20-Year	2.30	2.54	2.49	2.73	2.02	2.25	2.19	2.43
30-Year	2.32	2.57	2.52	2.76	2.05	2.29	2.23	2.47
40-Year	2.34	2.59	2.54	2.79	2.08	2.32	2.26	2.50
50-Year	2.35	2.60	2.55	2.80	2.10	2.34	2.28	2.52
75 Year	2.38	2.63	2.58	2.83	2.13	2.38	2.31	2.57

The factors shown below in Table 22 and Table 23 are recommended for use in the load rating calculations using the LFR approach which retain the target safety levels achieved in LRFR.

Table 22. Live Load Factors, $\gamma_{LL,HS20,Operating}$, for HS20 loading at Operating Level with the Multiple Presence Factor

Operating level	Single-Lane				2-Lane			
Return Period	Moment (SIB)	Shear (SIB)	Moment (QB)	Shear (QB)	Moment (SIB)	Shear (SIB)	Moment (QB)	Shear (QB)
5-Year	2.09	2.32	2.27	2.50	1.68	1.85	1.83	2.11

Table 23. Live Load Factors, $\gamma_{LL,HS20,Inventory}$, for HS20 Loading at Inventory Level with the Multiple Presence Factor

Inventory level	Single-Lane				2-Lane			
Return Period	Moment (SIB)	Shear (SIB)	Moment (QB)	Shear (QB)	Moment (SIB)	Shear (SIB)	Moment (QB)	Shear (QB)
10-Year	2.70	2.98	2.93	3.20	1.96	2.18	2.13	2.36
20-Year	2.76	3.04	2.99	3.27	2.02	2.25	2.19	2.43
30-Year	2.79	3.08	3.02	3.31	2.05	2.29	2.23	2.47
40-Year	2.81	3.10	3.04	3.34	2.08	2.32	2.26	2.50
50-Year	2.82	3.12	3.06	3.36	2.10	2.34	2.28	2.52
75 Year	2.86	3.16	3.09	3.40	2.13	2.38	2.31	2.57

Section 5 – Conclusions and Recommendations

This study evaluated the implemented testbed for automated enforcement of overweight trucks. A new A-WIM system was designed based on the experiences of the existing system. A new SHM system was also implemented in the testbed. The evaluations of the multiple systems in the testbed are presented by presenting the results of accuracy of different weighing sensors, and practices of automated enforcement. This section discussed the conclusions and recommendations from the project.

5.1. Findings and Conclusions

Following major findings and conclusions and be drawn from the study:

- On average, the IRD GVW measurements are overestimated in comparison to Kistler measurements, except for Class 7 trucks.
- The IRD GVW records have different errors for different GVW ranges. For instance, IRD tends to overestimate trucks below 60 kips and underestimate trucks over 60 kips.
- The correlation between GVW and acceleration is not strong. It shows that heavier trucks would not necessarily produce higher accelerations. Therefore, it is not recommended to establish a GVW limit on the bridge based on the acceleration measurements.
- A weak correlation was observed between acceleration and strain data, meaning that higher strains would be likely to be accompanied by higher accelerations.
- There is a clear trend between acceleration and speed - the higher the speed, the higher the acceleration response on QB-6M. This helps to explain why most of the events happen during the nighttime when there is no traffic jam.
- The “actual” success rate for the 1-hour test for all truck records and overweighted trucks is about 90%.

5.2. Recommendations

Based on the findings and conclusions, the recommendation for future study is summarized below:

- The IRD GVW error should be evaluated according to different GVW ranges.
- The Kistler system should be calibrated at least every 6 months.
- For the integration of WIM and ALPR data, more validation is needed. In addition, the solutions for missed cases need to be found.

References

American Association of State Highway and Transportation Officials (AASHTO), Standard Specifications for Highway Bridges, 17th Edition, Washington, D.C., 2002.

American Association of State Highway and Transportation Officials (AASHTO), LRFD Bridge Design Specifications, Ninth Edition, Washington, D.C., 2020.

American Association of State Highway and Transportation Officials (AASHTO), The Manual for Bridge Evaluation, Third Edition with 2020 Interim Revision, Washington, D.C., 2020.

Smith, K. D., Bruinsma, J. E., Wade, M. J., Chatti, K., Vandenbossche, J., & Yu, H. T. (2017). Using falling weight deflectometer data with mechanistic-empirical design and analysis, volume I (No. FHWA-HRT-16-009). United States. Federal Highway Administration.

Wassef, W. G., Kulicki, J. M., Nassif, H., Mertz, D., & Nowak, A. S. (2014). *Calibration of AASHTO LRFD concrete bridge design specifications for serviceability* (No. 201).